Chapter 3

Balanced dynamical theories

To a good first approximation the mature tropical cyclone consists of a horizontal quasi-symmetric circulation on which is superposed a thermally-direct vertical (transverse) circulation. These are sometimes referred to as the "primary circulation" and "secondary circulation", respectively. The former refers to the tangential flow rotating about the central axis, and the latter to the "in-up-and-out circulation" (low and middle level inflow, upper-level outflow). When these two components are combined, the picture emerges of air parcels spiralling inwards, upwards and outwards. The combined spiralling circulation is called energetically direct because the rising branch of the secondary circulation near the centre is warmer than the subsiding branch, which occurs at large radial distances (radii > 500 km). When warm air rises, potential energy is released.

In this chapter we examine the dynamics of the spiralling circulation of tropical cyclones on the basis of the physical laws governing fluid motion and thermodynamic processes that occur. For simplicity we study the dynamics of a stationary axisymmetric hurricane-like vortex. In Part II we consider the dynamics of tropical-cyclone motion and examine the asymmetric features of storms.

We start by giving an overall picture of the dynamics and then go into detail about particular important aspects. First we introduce the governing equations without making the assumption of axial symmetry.

3.1 The equations in cylindrical polar coordinates

Some basic properties of vortical flows that are relevant to tropical cyclones may be elucidated by considering the full equations of motion in cylindrical polar coordinates. The primitive equations of motion comprising the momentum equation, the continuity equation, the thermodynamic equation and the equation of state for frictionless motion in a rotating frame of reference on an f-plane may be expressed in cylindrical polar coordinates, (r, λ, z), as:

$$\frac{\partial u}{\partial t} + u\frac{\partial u}{\partial r} + \frac{v}{r}\frac{\partial u}{\partial \lambda} + w\frac{\partial u}{\partial z} - \frac{v^2}{r} - fv = -\frac{1}{\rho}\frac{\partial p}{\partial r}, \tag{3.1}$$

$$\frac{\partial v}{\partial t} + u\frac{\partial v}{\partial r} + \frac{v}{r}\frac{\partial v}{\partial \lambda} + w\frac{\partial v}{\partial z} + \frac{uv}{r} + fu = -\frac{1}{\rho r}\frac{\partial p}{\partial \lambda}, \tag{3.2}$$

$$\frac{\partial w}{\partial t} + u\frac{\partial w}{\partial r} + \frac{v}{r}\frac{\partial w}{\partial \lambda} + w\frac{\partial w}{\partial z} = -\frac{1}{\rho}\frac{\partial p}{\partial z} - g, \tag{3.3}$$

$$\frac{\partial \rho}{\partial t} + \frac{1}{r}\frac{\partial \rho r u}{\partial r} + \frac{1}{r}\frac{\partial \rho v}{\partial \lambda} + \frac{\partial \rho w}{\partial z} = 0, \tag{3.4}$$

$$\frac{\partial \theta}{\partial t} + u\frac{\partial \theta}{\partial r} + \frac{v}{r}\frac{\partial \theta}{\partial \lambda} + w\frac{\partial \theta}{\partial z} = \dot{\theta} \tag{3.5}$$

$$\rho = p_* \pi^{\frac{1}{\kappa}-1}/(R_d\theta) \tag{3.6}$$

where u, v, w are the velocity velocity components in the three coordinate directions, $\dot{\theta}$ is the diabatic heating rate $(1/c_p\pi)Dh/Dt$ (see Eq. 1.13), and $\pi = (p/p_*)^\kappa$ is the Exner function. The temperature is defined by $T = \pi\theta$.

Multiplication of Eq. (3.2) by r and a little manipulation leads to the equation

$$\frac{\partial M}{\partial t} + u\frac{\partial M}{\partial r} + \frac{v}{r}\frac{\partial M}{\partial \lambda} + w\frac{\partial M}{\partial z} = -\frac{1}{\rho}\frac{\partial p}{\partial \lambda}, \tag{3.7}$$

where

$$M = rv + \frac{1}{2}fr^2, \tag{3.8}$$

is the absolute angular momentum per unit mass of an air parcel about the rotation axis. If the flow is axisymmetric (and frictionless), the right-hand-side of (3.7) is zero and the absolute angular momentum is conserved as rings of air move radially.

3.2 The primary circulation

Important aspects of the basic structure of a mature tropical cyclone can be deduced from two simple equations that express an exact balance of forces in the vertical and radial directions. These equations enable one to develop a simple theory for the primary circulation. The equations are obtained directly from (3.1) - (3.6) assuming steady ($\partial/\partial t \equiv 0$) axisymmetric ($\partial/\partial\lambda \equiv 0$) flow with no diabatic heating ($\dot{\theta} = 0$) and no secondary circulation ($u = 0, w = 0$). In this case Eqs. (3.1) and (3.3) give,

$$\frac{1}{\rho}\frac{\partial p}{\partial r} = \frac{v^2}{r} + fv, \tag{3.9}$$

and

$$\frac{1}{\rho}\frac{\partial p}{\partial z} = -g, \tag{3.10}$$

while Eqs. (3.2) and (3.4) are identically satisfied. These equations apply to an steady, inviscid, freely-spinning vortex. Equation (3.9) expresses a balance between the radial pressure gradient and the centrifugal and Coriolis forces, each per unit mass, a state that we refer to as *gradient wind balance*. We call this equation the *gradient wind equation*. Equation (3.10) is just the hydrostatic equation, Eq. (1.4). The complete balance of forces is shown schematically in Fig. 3.1. A scale analysis carried out later shows that both the gradient wind equation and hydrostatic equation provide a good first approximation for representing the primary circulation of tropical cyclones, even in the presence of diabatic heating and a nonzero secondary circulation. Support for gradient wind balance is found also in analysis of aircraft observations in hurricanes.

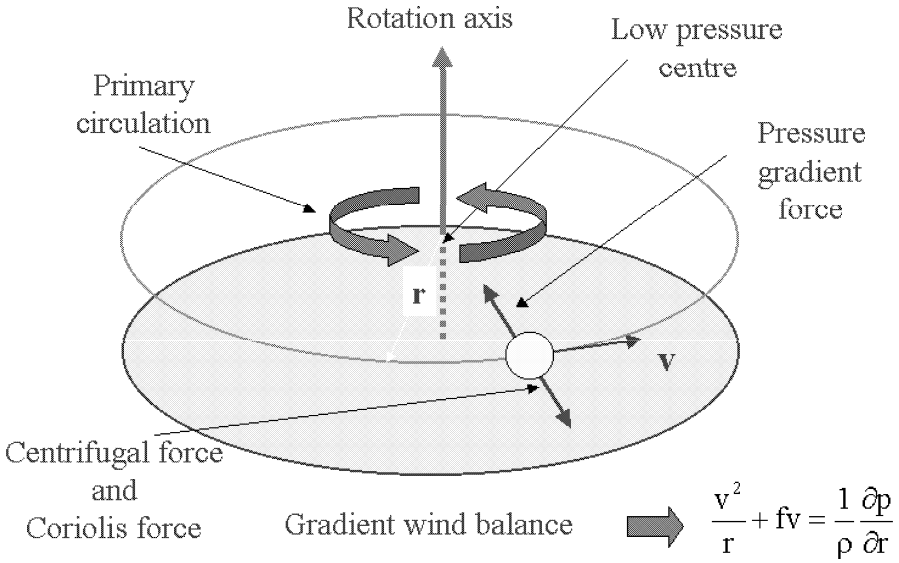

Figure 3.1: Schematic diagram illustrating the gradient wind force balance in the primary circulation of a tropical cyclone.

Taking $(\partial/\partial z)[\rho\times$ Eq. (3.9)$]$ and $(\partial/\partial r)[\rho\times$ Eq. (3.10)$]$ and eliminating the pressure we obtain the *thermal wind equation*

$$g\frac{\partial \ln \rho}{\partial r} + C\frac{\partial \ln \rho}{\partial z} = -\frac{\partial C}{\partial z}. \tag{3.11}$$

where

$$C = \frac{v^2}{r} + fv \tag{3.12}$$

denotes the sum of the centrifugal and Coriolis forces per unit mass. Equation (3.11) is a linear first-order partial differential equation for $\ln \rho$. The characteristics of the equation satisfy

$$\frac{dz}{dr} = \frac{C}{g}. \tag{3.13}$$

The characteristics are just the isobaric surfaces, because a small displacement (dr, dz) along an isobaric surface satisfies $(\partial p/\partial r)dr + (\partial p/\partial z)dz = 0$. Then, using the equations for hydrostatic balance ($\partial p/\partial z = -g\rho$) and gradient wind balance ($\partial p/\partial r = C\rho$) gives the equation for the characteristics. Alternatively, note that the pressure gradient per unit mass, $(1/\rho)(\partial p/\partial r, 0, \partial p/\partial z)$ equals $(C, 0, -g)$, which defines the "generalized gravitational vector", $\mathbf{g_e}$; see Fig. 3.2. The density variation along a characteristic is governed by the equation

$$\frac{d}{dr}\ln\rho = -\frac{1}{g}\frac{\partial C}{\partial z}. \tag{3.14}$$

Given the vertical density profile, $\rho_a(z)$, Eqs. (3.13) and (3.14) can be integrated inwards along the isobars to obtain the balanced axisymmetric density and pressure distributions. In particular, Eq. (3.13) gives the height of the pressure surface that has the value $p_a(z)$, say, at radius R.

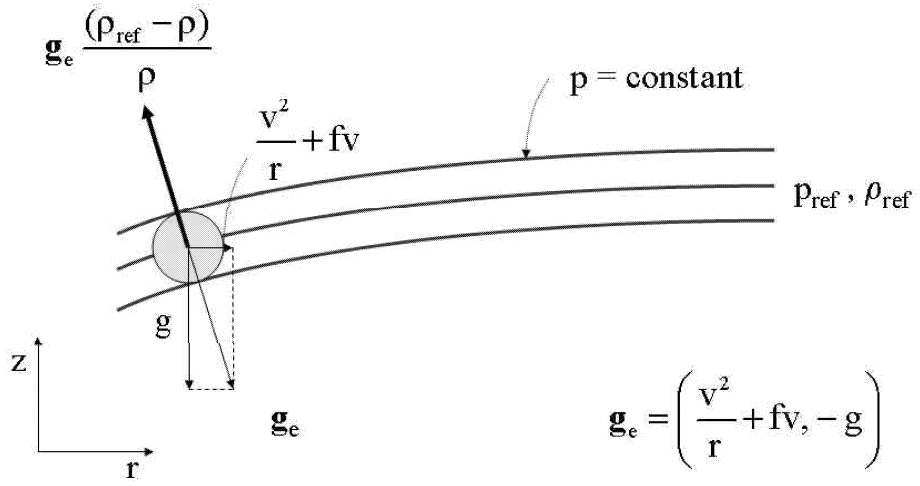

Figure 3.2: Schematic radial-height cross-section of isobaric surfaces in a rapidly-rotating vortex showing the forces on an air parcel including the gravitational force g, per unit mass, and the sum of the centrifugal and Coriolis forces $C = v^2/r + fv$ per unit mass. Note that the isobaric surfaces are normal to the local "generalized gravitational force" $\mathbf{g_e} = (C, 0, -g)$. The Archimedes force $-\mathbf{g_e}\rho_{ref}$ slopes upwards and inwards while the weight $\mathbf{g_e}\rho$ slopes downwards and outwards. Thus the net buoyancy force acting on the parcel per unit mass is $|\mathbf{g_e}|(\rho_{ref} - \rho)/\rho$ in the direction shown.

Since $\partial C/\partial z = (2v/r + f)(\partial v/\partial z)$, it follows from (3.14) that for a barotropic vortex ($\partial v/\partial z = 0$), ρ is constant along an isobaric surface, i.e. $\rho = \rho(p)$, whereupon, from the equation of state (1.8), T is a constant also, or more generally T_ρ if the air contains water substance: see Eq. (1.16).

The thermal wind equation (3.11), or equivalently Eq. (3.14), show that in a cyclonic vortex in the northern hemisphere ($v > 0$) with tangential wind speed that

decays with height ($\partial v/\partial z < 0$), $\log \rho$ and hence ρ decrease with decreasing radius along the isobaric surface. Thus the temperature and potential temperature increase and the vortex is warm cored (i.e. $\partial T/\partial r < 0$). This prediction of the thermal wind equation *is consistent with* the observation that tropical cyclones are warm-cored systems and that the tangential wind speed decreases with altitude. If the tangential wind speed were to increase with height ($\partial v/\partial z > 0$) the vortex would be cold cored. Note that the characteristics or isobars dip down as the axis is approached on account of Eq. (3.13). The reason for the warm core structure of tropical cyclones is discussed in Section 3.9.

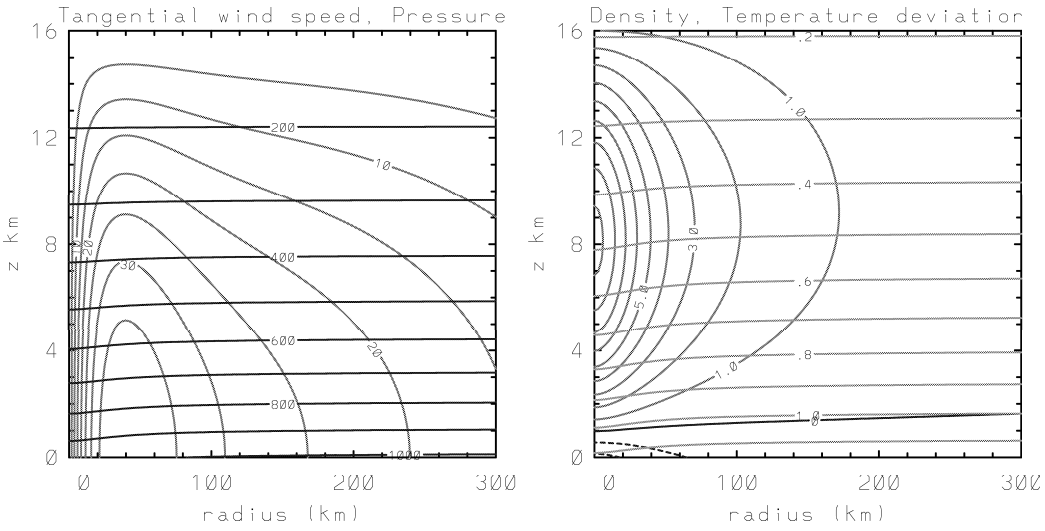

Figure 3.3: The primary circulation of a tropical cyclone.

Figure 3.3 shows an example of a calculation using the foregoing theory. The tangential wind field in Fig. 3.3a is broadly typical of that in a tropical cyclone. It is used to calculate the pressure field, shown also in this figure, as well as the density and temperature fields. The density field and the deviation in temperature from that at large radii are shown in Fig. 3.3b. Note that the isobars as well as the density contours dip down near the vortex axis. Temperatures in the vortex core region are warmer than at the same height in their environment except at low levels, where they are cooler.

The analysis above shows that any steady vortical flow with velocity field $\mathbf{u} = (0, v(r, z), 0)$ is a solution of the basic equation set (3.1) - (3.6), when the density field satisfies (3.10). The observational evidence that the primary circulation of a hurricane is approximately in gradient wind balance makes the foregoing analysis a good start in understanding the structure of this circulation. However the solution neglects the secondary circulation associated with nonzero u and w and it neglects the effects of heating and of friction near the sea surface. These are topics of subsequent subsections.

Exercise 3.1 Assuming the most general form of the mass conservation equation:

$$\frac{\partial \rho}{\partial t} + \frac{1}{r}\frac{\partial (\rho r u)}{\partial r} + \frac{1}{r}\frac{\partial (\rho v)}{\partial \lambda} + \frac{\partial (\rho w)}{\partial z} = 0,$$

show that the absolute angular momentum per unit volume,

$$M_v = \rho \left(rv + \frac{1}{2} f r^2 \right),$$

satisfies the equation:

$$\frac{\partial M_v}{\partial t} + \frac{1}{r}\frac{\partial (r u M_v)}{\partial r} + \frac{1}{r}\frac{\partial (v M_v)}{\partial \lambda} + \frac{\partial (w M_v)}{\partial z} = -\frac{\partial p}{\partial \lambda}.$$

Exercise 3.2 Show that Eq. (3.10) may be reformulated as

$$g\frac{\partial (\ln \chi)}{\partial r} + C\frac{\partial (\ln \chi)}{\partial z} = -\frac{\partial C}{\partial z}. \tag{3.15}$$

where $\chi = 1/\theta$.

Exercise 3.3 Show that in terms of the Exner function, Eqs. (3.9) and (3.10) may be written as

$$\chi C = c_p \frac{\partial \pi}{\partial r} \quad \text{and} \quad -\chi g = c_p \frac{\partial \pi}{\partial z}, \tag{3.16}$$

respectively.

3.3 Stability

Having shown that any steady vortical flow with velocity field $\mathbf{u} = (0, v(r, z), 0)$ is a solution of the basic equations, it is appropriate to ask under what circumstances such solutions are stable. We consider here local stability based on parcel arguments. Other aspects of vortex stability will be discussed in Part II.

3.3.1 Barotropic vortices

We begin by considering a barotropic vortex rotating with tangential velocity $v(r)$ in a homogeneous fluid. Solid body rotation is the special case $v(r) = \Omega r$, where Ω is the constant angular velocity. The approach is to investigate the forces acting on a fluid parcel that is displaced radially outwards from A at radius r_1 to B at radius r_2 in Fig. (3.4). Assuming frictional torques can be neglected, the parcel conserves its absolute angular momentum so that its velocity v' at B is given by

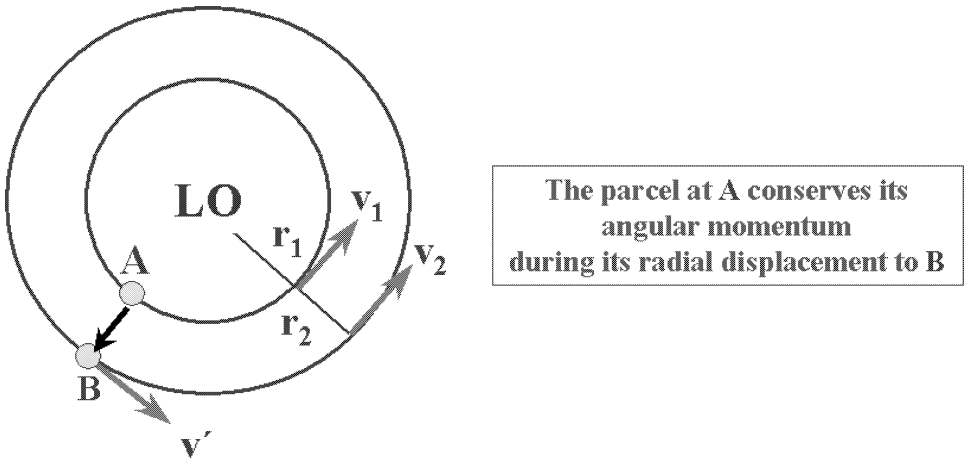

Figure 3.4: Radial displacement of an air parcel in a rotating flow.

$$r_2 v' + \frac{1}{2} f r_2^2 = r_1 v_1 + \frac{1}{2} f r_1^2, \quad \text{or} \quad v' = \frac{r_1}{r_2} v_1 + \frac{1}{2} \frac{f}{r_2} (r_1^2 - r_2^2) \tag{3.17}$$

Other parcels at the same radius as B have a velocity v_2 that is different, in general, from v'. In equilibrium, these parcels are in a balanced state in which the radially-inward pressure gradient force they experience is exactly balanced by the outward centrifugal force; i.e.,

$$\frac{1}{\rho} \frac{dp}{dr}\Big]_{r=r_2} = \frac{v_2^2}{r_2} + f v_2. \tag{3.18}$$

It is assumed that the disturbance brought about by the displaced parcel at radius r_2 can be neglected. Now, the displaced parcel will experience the same radial pressure gradient as other parcels at radius r_2, but since it rotates with velocity v', the sum of the centrifugal and Coriolis forces acting on it are $v'^2/r_2 + f v'$. Therefore, the displaced parcel experiences an *outward* force per unit mass,

$$F = \text{centrifugal} + \text{Coriolis force} - \text{radial pressure gradient}$$

$$= \frac{v'^2}{r_2} + f v' - \frac{1}{\rho} \frac{\partial p}{\partial r}\Big]_{r=r_2}$$

Using (3.17) and (3.18), this expression can be written after a little algebra (see Exercise 3.4)

$$F = \frac{1}{r_2^3} \left[(r_1 v_1 + \frac{1}{2} r_1^2 f)^2 - (r_2 v_2 + \frac{1}{2} r_2^2 f)^2 \right]. \tag{3.19}$$

Therefore an air parcel displaced outwards experiences an inward force (i. e. a restoring force) that is proportional to the difference in the absolute angular momentum

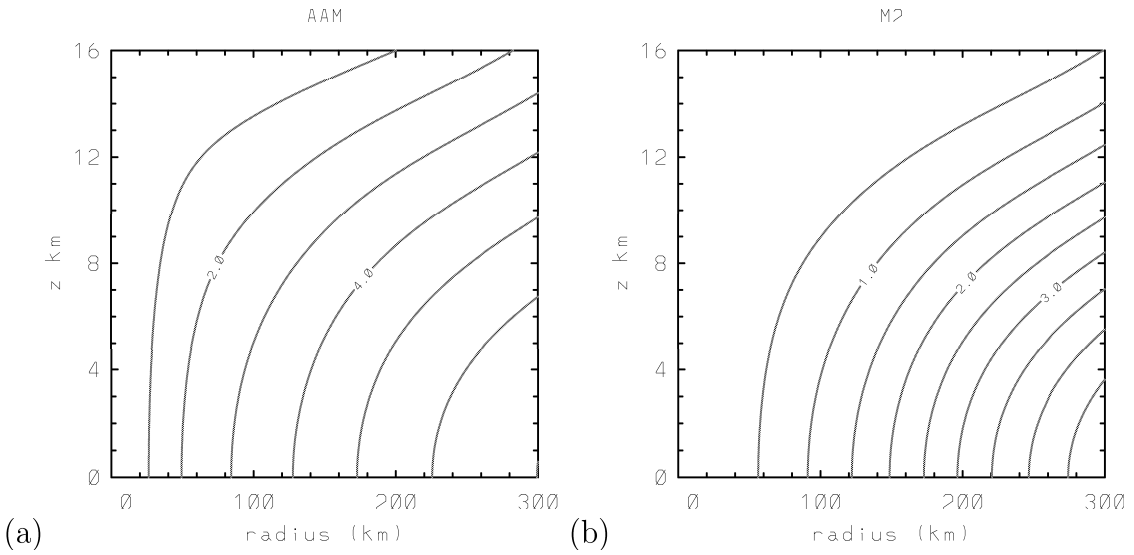

Figure 3.5: Height-radius distributions of the quantities (a) M (Unit $\times 10^6$ s^{-2}) and (b) M^2 (Unit $\times 10^{13}$ s^{-2}) for the vortex in Fig. 3.3.

squared between the two radii. Height-radius distributions of the quantities M, and M^2 for the *baroclinic* vortex in Fig. 3.3 are shown in Fig. 3.5.

In the special case of solid body rotation, $v = \Omega r$, and for a small displacement from radius $r_1 = r$ to $r_2 = r + r'$, (3.19) gives

$$F \approx -4(\Omega + \frac{1}{2}f)^2 r' \tag{3.20}$$

Thus, an air parcel displaced outwards experiences an inward restoring force, proportional to the displacement and to the square of the absolute angular frequency $\Omega + \frac{1}{2}f$. Likewise, a parcel displaced inwards experiences an outward force, again a restoring force. This result is in direct analogy with the restoring force that acts on a fluid parcel when it is displaced vertically in a stably-stratified, non-rotating fluid. Note that if the rotation rate $\Omega >> \frac{1}{2}f$, such as in a rotating tank in the laboratory, the rotation of the coordinate system can be neglected and $F \approx -4\Omega^2 r'$.

The presence of a restoring force when a air parcel is displaced radially in a rapidly-rotating fluid leads to the concept of *inertial stiffness*. The larger the rotation rate, the harder it is to displace an air parcel radially.

Exercise 3.4 Verify that

$$\frac{v'^2}{r_2} + fv' - \frac{1}{\rho}\frac{\partial p}{\partial r}\Big]_{r=r_2} = \frac{1}{r_2^3}\left[(r_1 v_1 + \frac{1}{2}r_1^2 f)^2 - (r_2 v_2 + \frac{1}{2}r_2^2 f)^2\right],$$

and show that in the case of solid body rotation, $v = \Omega r$, the expression for F in (3.19) reduces to that in (3.20).

We can reformulate the problem considered above in a way that can be naturally extended to baroclinic vortices (see next subsection). First note that $C = v^2/r + fv$ and $M = rv + \frac{1}{2}fr$ are related by the formula

$$C = \frac{1}{r^3}\left(M^2 - \frac{1}{4}r^2 f^2\right) \tag{3.21}$$

Now the net outward radial force acting on the displaced air parcel at radius $r + r'$ is just the sum of the centrifugal and Coriolis forces, $C_{parcel}(r + r')$, minus the radial pressure gradient at that radius, which is equal to $C(r + r')$. The latter may be written approximately as

$$C(r + r') = C(r) + \frac{dC}{dr}r' \,, \tag{3.22}$$

and using (3.21),

$$\frac{dC}{dr} = \frac{1}{r^3}\frac{dM^2}{dr} - \frac{3}{r^4}M^2 + \frac{1}{4}\frac{f^2}{r^2} \,. \tag{3.23}$$

Similarly,

$$C_{parcel}(r + r') = C_{parcel}(r) + \frac{dC_{parcel}}{dr}r', \tag{3.24}$$

but since M is conserved during the radial displacement,

$$\frac{d}{dr}C_{parcel} = -\frac{3}{r^4}M^2 + \frac{1}{4}\frac{f^2}{r^2}. \tag{3.25}$$

Also $C_{parcel}(r) = C(r)$ because the parcel is in equilibrium at radius r before it is displaced. Using Eqs. (3.22) - (3.25), the net outward force per unit mass acting on the displaced parcel is

$$C_{parcel}(r + r') - C(r + r') = -\frac{1}{r^3}\frac{dM^2}{dr}r'. \tag{3.26}$$

This expression enables us to establish a criterion for the stability of a general rotating flow $v(r)$, analogous to the criterion in terms of $\mathrm{sgn}(N^2)$ for the stability of a density stratified fluid. It follows from (3.26) that a general swirling flow $v(r)$ is stable, neutral or unstable if the radial gradient of the square of the absolute angular momentum is positive, zero, or negative.

3.3.2 Baroclinic vortices

The foregoing stability theory can be readily extended to the case of a balanced baroclinic vortex in a stably-stratified atmosphere. We consider then the displacement of an air parcel from a point A at radius r and height z to a neighbouring point B with coordinates $(r + r', z + z')$ (see Fig. 3.6). The radial force acting on the displaced

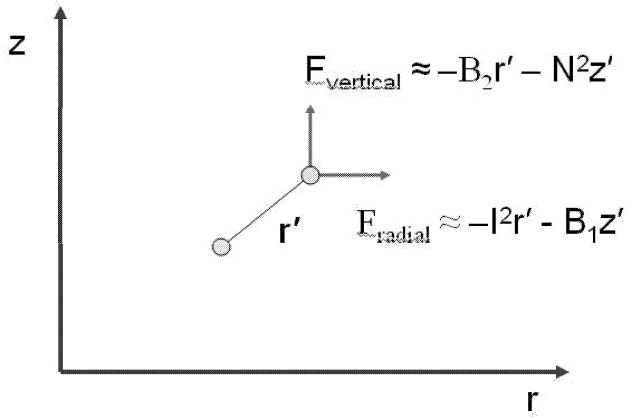

Figure 3.6: The radial and vertical displacement of an air parcel in a rotating flow is accompanied by the restoring forces shown. For a vortex in which the tangential wind speed decreases with height, the quantities B_1 and B_2 are negative (see e.g. Fig. 3.7) and in this case give contributions in the directions of the component displacements. Under certain circumstances they might lead to instability as discussed in the text.

air parcel is again the difference between $C_{parcel}(r+r', z+z')$ and $C(r+r', z+z')$ but now

$$C(r+r', z+z') = C(r) + \frac{\partial C}{\partial r} r' + \frac{\partial C}{\partial z} z',$$

and there is a similar expression for $C_{parcel}(r+r', z+z')$. These expressions differ only through the terms involving gradients of M^2, which are again zero in the case of C_{parcel}. Then the net radial force acting on the displaced air parcel is approximately

$$C_{parcel}(r+r', z+z') - C(r+r', z+z') = -\frac{1}{r^3}\frac{\partial M^2}{\partial r} r' - \frac{1}{r^3}\frac{\partial M^2}{\partial z} z'. \tag{3.27}$$

The radial component of Newton's second law for the air parcel then takes the form

$$\frac{\partial^2 r'}{\partial t^2} = -\frac{1}{r^3}\frac{\partial M^2}{\partial r} r' - \frac{1}{r^3}\frac{\partial M^2}{\partial z} z'. \tag{3.28}$$

The vertical component of Newton's second law may be obtained in an entirely analogous way, starting with a small vertical displacement z' and

$$\frac{\partial^2 z'}{\partial t^2} = b_{parcel}(r+r', z+z') - b(r+r', z+z'), \tag{3.29}$$

where $b_{parcel}(r+r', z+z')$ is the buoyancy of the displaced air parcel at B, obtained by assuming that the potential temperature[1] is conserved and $b(r+r', z+z')$ is the

[1]Or the equivalent potential temperature is conserved for saturated ascent.

buoyancy of all other air parcels at $(r+r', z+z')$. In terms of potential temperature, θ, the buoyancy b may be written as:

$$b = g\left(\frac{\theta}{\bar{\theta}} - 1 + (1-\kappa)\frac{p'}{\bar{p}}\right), \tag{3.30}$$

where $\bar{p}$ and $\bar{\theta}$ are the reference pressure and potential temperature, assumed here to be the values of these quantities at large radial distances at height z, p' is the pressure perturbation at this height and $\kappa = R_d/c_p$ (see Eq. 1.29). Then

$$b_{parcel}(r+r', z+z') - b(r+r', z+z') = -\frac{g}{\bar{\theta}}\frac{\partial\theta}{\partial r}r' - \frac{g}{\bar{\theta}}\frac{\partial\theta}{\partial z}z', \tag{3.31}$$

and (3.29) reduces to

$$\frac{\partial^2 z'}{\partial t^2} = -\frac{g}{\bar{\theta}}\frac{\partial\theta}{\partial r}r' - \frac{g}{\bar{\theta}}\frac{\partial\theta}{\partial z}z'. \tag{3.32}$$

Equations (3.28) and (3.32) are a pair of ordinary differential equations for the parcel displacement (r', z'). Define

$$I^2 = \frac{1}{r^3}\frac{\partial M^2}{\partial r}, \qquad N^2 = \frac{g}{\bar{\theta}}\frac{\partial\theta}{\partial z},$$

$$B_1 = \frac{1}{r^3}\frac{\partial M^2}{\partial z}, \qquad B_2 = \frac{g}{\bar{\theta}}\frac{\partial\theta}{\partial r}. \tag{3.33}$$

The height-radius distributions of the quantities N^2, I^2, B_1 and B_2 for the vortex in Fig. 3.3 are shown in Fig. 3.7. Note that for a vortex in which the tangential wind speed decreases with height, B_1 and B_2 are typically negative and contribute to force perturbations in the direction of the displacement as seen in Fig. 3.6.

If the quantities N^2, I^2, B_1 and B_2 are appreciably constant on the scale of a parcel displacement, Eqs. (3.28) and (3.32) have solutions of the form $(r', z') = (r'_0, z'_0)\exp(i\omega t)$, where r'_0, z'_0 and ω are constants and the frequency ω satisfies the pair of equations:

$$\begin{aligned}(I^2 - \omega^2)r'_0 + B_1 z'_0 &= 0,\\ B_2 r'_0 + (N^2 - \omega^2)z'_0 &= 0.\end{aligned} \tag{3.34}$$

These have a solution for (r'_0, z'_0) only if

$$(N^2 - \omega^2)(I^2 - \omega^2) - B_1 B_2 = 0.$$

or

$$\omega^4 - \omega^2(N^2 + I^2) + N^2 I^2 - B_1 B_2 = 0. \tag{3.35}$$

Then

$$\omega^2 = \frac{1}{2}\left[(N^2 + I^2) \pm \sqrt{\{(N^2 + I^2)^2 - 4(N^2 I^2 - B_1 B_2)\}}\right]. \tag{3.36}$$

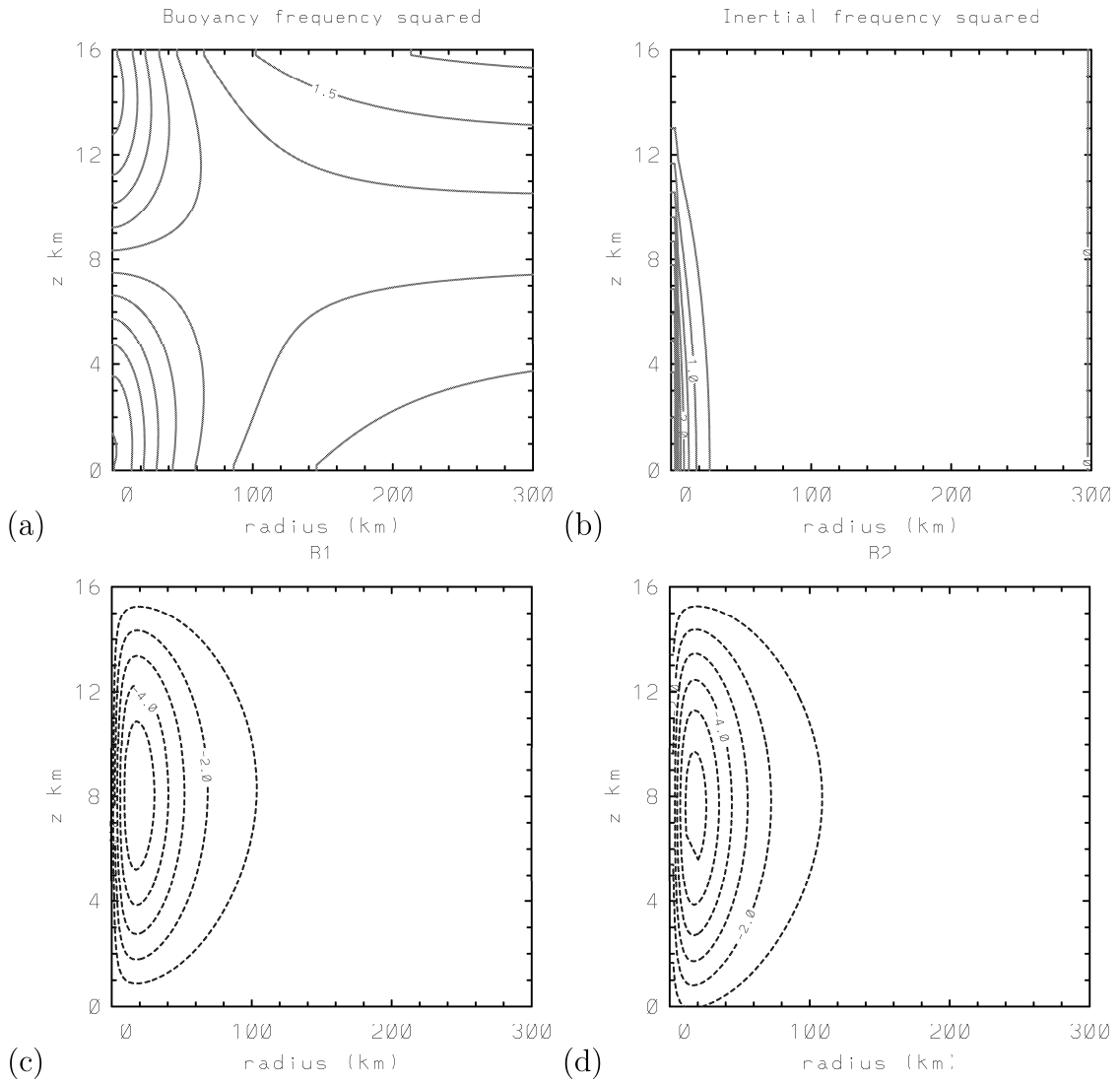

Figure 3.7: Height-radius distributions of the quantities (a) N^2 (Unit $\times 10^{-4}$ s^{-2}), (b) I^2 (Unit $\times 10^{-5}$ s^{-2}), (c) B_1 (Unit $\times 10^{-6}$ s^{-2}), (d) B_2 (Unit as for B_1).

Note that the expression under the square-root sign can be rewritten as $(N^2 - I^2)^2 + 4B_1B_2$ and it is always positive if $B_1B_2 > 0$ (see Exercise 3.5). Then the solutions for ω^2 are both positive provided that the magnitude of $(N^2 + I^2)$ is larger than the square root term, i.e. if the discriminant $\Delta = (N^2 + I^2)^2 - [(N^2 - I^2)^2 - 4B_1B_2] = 4(N^2I^2 - B_1B_2)$ is positive. In this case the parcel oscillates along the (r_0', z_0') with frequency ω given by (3.36) and the flow is *stable*. On the other hand, if $\Delta < 0$, one solution for ω^2 is negative. In this case, two solutions for ω are imaginary and one of these gives an exponentially growing solution for the parcel displacement. In this case a displaced parcel continues to move away from its initial position and the displacement is therefore unstable. We refer to this situation as

symmetric instability. It is left for the reader to show that the sign of Δ is equal to the sign of the *potential vorticity*, q, divided by the *absolute angular rotation rate* $\frac{1}{2}\xi = V/r + \frac{1}{2}f$ (see Exercise 3.3). Note that $V > -\frac{1}{2}fr$ is required for gradient wind balance to exist in anticyclonic flow ($\partial p/\partial r > 0$)[2]. The height-radius distributions of the the discriminant Δ for the vortex in Fig. 3.3 is shown in Fig. 3.8.

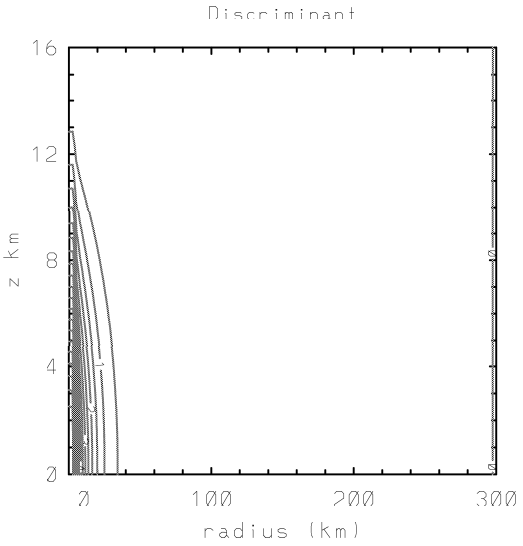

Figure 3.8: Height-radius distributions of the quantities (a) M (Unit $\times 10^6$ s^{-2}) and (b) M^2 (Unit $\times 10^{13}$ s^{-2}) for the vortex in Fig. 3.3.

The trajectory of a particle can be obtained as follows. Suppose that the flow is symmetrically stable and that the initial parcel displacement is to the point (r'_0, z'_0). Let ω_1 and ω_2 be the eigenfrequencies given by Eq. (3.36). From (3.34), the corresponding eigenvectors are: $(1, (\omega_1^2 - I^2)/B_1)$ and $(1, (\omega_2^2 - I^2)/B_1)$. Then the parcel displacement at time t may be written as

$$\begin{aligned}(r'(t), z'(t)) = (1, (\omega_1^2 - I^2)/B_1)(c_{1+}e^{i\omega_1 t} + c_{1-}e^{-i\omega_1 t}) \\ +(1, (\omega_2^2 - I^2)/B_1)(c_{2+}e^{i\omega_2 t} + c_{2-}e^{-i\omega_2 t}),\end{aligned} \tag{3.37}$$

where $c_{1\pm}$ and $c_{2\pm}$ are four constants. At $t = 0$, $(r'(t), z'(t)) = (r'_0, z'_0)$ and we assume that the particle has no initial motion: $(dr'/dt, dz'/dt) = (0, 0)$. These conditions determine $c_{1\pm}$ and $c_{2\pm}$. The second condition gives us $c_{1-} = c_{1+} = \frac{1}{2}c_1$ and $c_{2-} = c_{2+} = \frac{1}{2}c_2$ so that if both values of ω^2 are positive, Eq. (3.38) becomes

$$(r'(t), z'(t)) = (1, (\omega_1^2 - I^2)/B_1)(c_1 \cos(\omega_1 t)) + (1, (\omega_2^2 - I^2)/B_1)(c_2 \cos(\omega_2 t)). \tag{3.38}$$

[2]Solving the equation for gradient wind balance gives: $v = -\frac{1}{2}rf + \sqrt{[\frac{1}{4}r^2f^2 + (1/\rho)(\partial p/\partial r)]}$, where the positive sign is chosen so that the expression reduces to that for geostrophic balance at large radial distances. Then v cannot exceed $\frac{1}{2}rf$ in magnitude. If, however, $\partial p/\partial r = 0$, a balanced solution is possible with $v = -rf$ in which $C = 0$ and the Coriolis force is balanced by the centrifugal force.

This equation gives $c_1 + c_2 = r'_0$ and $c_1(\omega_1^2 - I^2) + c_2(\omega_2^2 - I^2) = B_1 z'_0$, from which,

$$c_1 = [(\omega_2^2 - I^2)r'_0 - B_1 z'_0]/(\omega_2^2 - \omega_1^2) \tag{3.39}$$

and

$$c_2 = [B_1 z'_0 - (\omega_1^2 - I^2)r'_0]/(\omega_2^2 - \omega_1^2). \tag{3.40}$$

Finally

$$r'(t) = \frac{(\omega_2^2 - I^2)r'_0 - B_1 z'_0}{(\omega_2^2 - \omega_1^2)} \cos(\omega_1 t) + \frac{B_1 z'_0 - (\omega_1^2 - I^2)r'_0}{(\omega_2^2 - \omega_1^2)} \cos(\omega_2 t) \tag{3.41}$$

and

$$z'(t) = \frac{(\omega_2^2 - I^2)}{B_1} \frac{(\omega_1^2 - I^2)r'_0 - B_1 z'_0}{(\omega_2^2 - \omega_1^2)} \cos(\omega_1 t) + \frac{(\omega_2^2 - I^2)}{B_1} \frac{B_1 z'_0 - (\omega_1^2 - I^2)r'_0}{(\omega_2^2 - \omega_1^2)} \cos(\omega_2 t). \tag{3.42}$$

An example of an air-parcel trajectory in a symmetrically-stable rotating shear flow is shown in Fig. 3.9a and one that is in a symmetrically-unstable flow is shown in Fig. 3.9b.

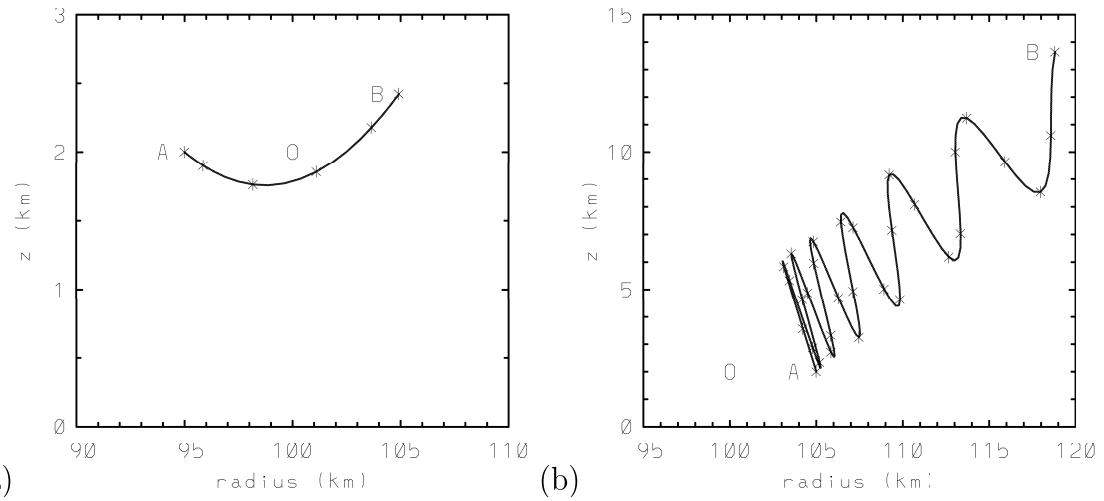

Figure 3.9: Displacement of an air parcel in a rotating shear flow that is (a) symmetrically-stable, and (b) symmetrically-unstable. In each case the parcel is initially displaced from O to A. The subsequent track is the blue line from A to B. The '*' marks show locations every two minutes. For these calculations we take N^2, I^2, B_1, and B_2 to be constants. In each case $N = 1.0 \times 10^{-2}$ s^{-1} and $I = 5.0 \times 10^{-3}$ s^{-1}. In (a), $B_1 = B_2 = 3.27 \times 10^{-6}$ s^{-2}, and in (b) $B_1 = B_2 = -1.01 \times NI$.

Exercise 3.5 Show that

$$I^2 = \xi(\zeta + f)$$

and

$$B_1 = \xi \frac{\partial v}{\partial z}$$

where

$$\xi = \frac{2v}{r} + f.$$

Show also that

$$M^2 = r^3 C - \frac{1}{4} f^2 r^4$$

and that

$$B_2 = -\frac{g\theta}{\bar{\theta}} \left(\frac{\partial}{\partial r} \ln \rho + \frac{(1-\kappa)}{R_d T} C \right)$$

Exercise 3.6 Starting with the expressions for B_1 and B_2 in the previous exercise, show that

$$B_1 B_2 = \left(\xi \frac{\partial v}{\partial z} \right)^2 \frac{\theta}{\bar{\theta}} + \xi \frac{\partial v}{\partial z} \frac{\theta}{\bar{\theta}} \frac{\kappa C}{H_s}.$$

and that within the framework of the Boussinesq approximation $B_1 = B_2$.

Exercise 3.7 Show that the potential vorticity for the vortex $v(r, z)$ is

$$PV = \frac{1}{\rho} \left(-\frac{\partial v}{\partial z} \frac{\partial \theta}{\partial r} + (\zeta + f) \frac{\partial \theta}{\partial z} \right).$$

Deduce that

$$PV = \frac{\bar{\theta}}{\rho g \xi} \left(I^2 N^2 - B_1 B_2 \right).$$

Exercise 3.8 Show that $\nabla\theta \wedge \nabla M$ is proportional to the potential vorticity, i.e. to $I^2 N^2 - B_1 B_2$. Show that this quantity is negative when the θ-surfaces are more steeply inclined to the horizontal than the M-surfaces. Note that this configuration of M- and θ-surfaces is therefore a condition for symmetric instability. Note also that the alignment of the M- and θ-surfaces implies zero potential vorticity.

Exercise 3.9 Show that in the symmetrically-unstable case, the terms involving $\cos(\omega_2 t)$ in Eqs. (3.41) and (3.42) must be replaced with $\cosh(\omega_2^* t)$, where $\omega_2^{*2} = -\omega_2$.

3.4 Generalized buoyancy

The expression for buoyancy (1.26) is valid also in a rapidly rotating vortex, but as shown in section 3.2, there exists then a radial component of buoyancy as well. When clouds are involved it may be advantageous to include the drag of hydrometeors in the definition of buoyancy. This may be done by using the density temperature given by Eq. (1.16) in place of the temperature for dry air, or the virtual temperature for moist air.

In a rapidly-rotating, axisymmetric vortex, an air parcel experiences not only the gravitational force, but also the radial force $C = v^2/r + fv$, where v is the tangential wind component at radius r. If the vortex is in hydrostatic and gradient wind balance, the isobaric surfaces slope in the vertical and are normal to the effective gravity, $\mathbf{g_e} = (C, 0, -g)$, expressed in cylindrical coordinates (r, λ, z) (see Fig. 3.2). The Archimedes force acting on the parcel is then $-\mathbf{g_e}\rho_{ref}$ and the effective weight of the parcel is $\mathbf{g_e}\rho$, where ρ_{ref} is now the far-field (reference-) density *along the same isobaric surface as the parcel*. Accordingly, we may define a *generalized buoyancy force per unit mass*:

$$\mathbf{b} = \mathbf{g_e}\frac{\rho - \rho_{ref}}{\rho}, \tag{3.43}$$

analogous to the derivation of (1.26). Note that unless[3] $v(v + rf) < 0$, air parcels that are lighter than their environment have an inward-directed component of generalized buoyancy force as well as an upward component, while heavier parcels have an outward component as well as a downward component. This result provides the theoretical background for a *centrifuge*. A centrifuge is a device used to separate lighter from heavier substances by rotating them rapidly in some container.

3.5 Scale analysis

It is instructive to perform a scale analysis of the dynamical equations (3.1) - (3.3) and continuity equation (3.4). It suffices to assume that the air is homogeneous and frictionless and that the motion is axisymmetric. In later chapters we redo this analysis for nonaxisymmetric flows and those in which friction is important. We define velocity scales (U, V, W) for (u, v, w), length scales (R, Z) for (r, z), a time scale T for t, a scale Δp for changes in pressure, p. We define two nondimensional parameters: a *swirl parameter* $S = U/V$ and a *Rossby number* $Ro = V/fR$. We assume also an *advective time scale* for the secondary circulation $T = U/R$. (for axisymmetric motions the time-scale V/R is not relevant). Then the terms in Eqs. (3.1) to (3.4) have scales as shown in Table 3.1.

From line (1) in Table 3.1 we see that the continuity equation (3.4) implies that $W/Z = U/R$, a result that is used to simplify the scalings. We divide terms in line

[3] If $v(v + rf) < 0$, C is directed inwards. Then, in the Northern Hemisphere, $-rf < v < 0$, i.e. the tangential flow is anticyclonic and relatively weak.

Table 3.1: Scaling of the terms in Eqs. (3.1) to (3.4), beginning with the last of these.

continuity

$\frac{1}{r}\frac{\partial \rho r u}{\partial r}$	$\frac{\partial \rho w}{\partial z}$	(3.4)
$\rho\frac{U}{R}$	$\rho\frac{W}{Z}$	(1)

u-momentum

$\frac{\partial u}{\partial t}$	$+u\frac{\partial u}{\partial r}$	$+w\frac{\partial u}{\partial z}$	$-\frac{v^2}{r}$	$-fv$	$=$	$-\frac{1}{\rho}\frac{\partial p}{\partial r}$	(3.1)
$\frac{U}{T}$	$\frac{U^2}{R}$	$W\frac{U}{Z}$	$\frac{V^2}{R}$	fV		$\frac{\Delta p}{\rho R}$	(2a)
S^2	S^2	S^2	1	$\frac{1}{Ro}$		$\frac{\Delta p}{\rho V^2}$	(2b)

v-momentum

$\frac{\partial v}{\partial t}$	$+u\frac{\partial v}{\partial r}$	$+w\frac{\partial v}{\partial z}$	$+\frac{uv}{r}$	$+fu$	$=$		(3.2)
$\frac{V}{T}$	$U\frac{V}{R}$	$\frac{WV}{Z}$	$\frac{UV}{R}$	fU			(3a)
S	S	S	S	$\frac{S}{Ro}$			(3b)

w-momentum

$\frac{\partial w}{\partial t}$	$+u\frac{\partial w}{\partial r}$	$+w\frac{\partial w}{\partial z}$			$=$	$-\frac{1}{\rho}\frac{\partial p}{\partial z}$ - g	(3.3)
$\frac{W}{T}$	$U\frac{W}{R}$	$W\frac{W}{Z}$				$\frac{\Delta p}{\rho Z}$ g	(4a)
$\frac{WU}{Rg}$	$\frac{UW}{Rg}$	$\frac{WU}{Rg}$				$\frac{\Delta p}{\rho g Z}$ 1	(4b)

(2a) by V^2/R to obtain those in line (2b) and divide terms in line (3a) by UV/R to obtain those in line (3b). The terms in line (4a) are divided by g to obtain those in line (4b). The terms in lines (b) are then nondimensional.

It follows from line (2b) in Table 3.1 that for low swirl ratio, $S << 1$, the radial momentum equation is closely approximated by the gradient wind equation (Note that if the pressure term had a larger order of magnitude than the sum of the centrifugal and Coriolis terms, it would drive a radial acceleration that would eventually violate the assumption that $S << 1$. Line (3b) in the table shows that all the nonlinear terms in the azimuthal momentum equation are of the same order of magnitude. These are dominant if $Ro >> 1$, but the Coriolis term is of equal importance[4] if $Ro << 1$.

Line (4b) in Table 3.1 shows that the ratio of the acceleration terms in the vertical momentum equation to the gravitational acceleration is WU/Rg. Typical scales for a tropical cyclone are $U \leq 20$ m s^{-1}, $W \leq 1$ m s^{-1}, $R \geq 50$ km and $g \sim 10$ m s^{-2}. Then $WU/Rg \leq 4 \times 10^{-5}$. We conclude that the motion on these scales is very close to hydrostatic balance with the vertical pressure gradient term in the momentum equation balancing the gravitational acceleration, i.e. Eq. (3.3) is closely approximated by (3.10). This means that the theory for the primary circulation worked out in section 3.2 should be a good approximation to reality.

3.6 The tropical cyclone eye

Observations show that the eye is a cloud free region surrounding the storm axis where the air temperatures are warmest. Therefore, it would be reasonable to surmise that the air within it has undergone descent during the formative stages of the cyclone, and that possibly it continues to descend. The question then is: why doesn't the inflowing air spiral in as far as the axis of rotation. We address this question later, but note here that eye formation is consistent with other observed features of the tropical cyclone circulation. Assuming that the primary circulation is in gradient wind balance, we may integrate Eq. (3.9) with radius to obtain a relationship between the pressure perturbation at a given height z on the axis to the tangential wind field distribution, i.e:

$$p(0,z) = p_a(z) - \int_0^\infty \rho \left(\frac{v^2}{r} + fv \right) dr, \tag{3.44}$$

where $p_a(z) = p(\infty, z)$ is the environmental pressure at the same height. Differentiating Eq. (3.44) with respect to height and dividing by the density gives the perturbation pressure gradient per unit mass along the vortex axis:

$$-\frac{1}{\rho}\frac{\partial (p - p_a)}{\partial z} = -\frac{1}{\rho}\frac{\partial}{\partial z}\int_0^\infty \rho \left(\frac{v^2}{r} + fv \right) dr. \tag{3.45}$$

[4]We cannot argue that it is dominant, since then the other terms would be negligible, but then we would conclude that $fu = 0$!

Observations in tropical cyclones show that the tangential wind speed decreases with height above the boundary layer and that the vortex broadens with height in the sense that the radius of the maximum tangential wind speed increases with altitude (see Fig. 2.11). This behaviour, which is consistent with outward-slanting absolute angular momentum surfaces as discussed above, implies that the integral on the right-hand-side of Eq. (3.45) decreases with height. Then Eq. (3.45) shows that there must be a downward-directed perturbation pressure gradient force per unit mass along the vortex axis. If unopposed, this perturbation pressure gradient would drive subsidence along and near to the axis to form the eye. However, as air subsides, it is compressed and warms relative to air at the same level outside the eye and thereby becomes locally buoyant (i.e. relative to the air outside the eye). In reality this upward buoyancy approximately balances the downward directed (perturbation) pressure gradient so that the actual subsidence results from a small residual force. In essence the flow remains close to hydrostatic balance.

As the vortex strengthens, the downward pressure gradient must increase and the residual force must be downwards to drive further subsidence. On the other hand, if the vortex weakens, the residual force must be upwards, allowing the air to re-ascend. In the steady state, the residual force must be zero and there is no longer a need for up- or down motion in the eye, although, in reality there may be motion in the eye associated with turbulent mixing across the eyewall or with asymmetric instabilities within the eye.

It is not possible to measure the vertical velocity that occur in the eye, but one can make certain inferences about the origin of air parcels in the eye from their thermodynamic characteristics, which can be measured.

The above arguments are incomplete as they are based on the assumption of exact balance and cannot account for the residual force. A more complete theory is given below.

3.7 The secondary circulation

If the vortex is axisymmetric and in approximate geostrophic and hydrostatic balance, we can derive an equation for the streamfunction, ψ, of the secondary circulation, i.e. the circulation in a vertical plane. This streamfunction is such that

$$u = -\frac{1}{r\rho}\frac{\partial \psi}{\partial z} \qquad w = \frac{1}{r\rho}\frac{\partial \psi}{\partial r}. \tag{3.46}$$

which ensures that the continuity equation (3.4), is satisfied. The equation for ψ follows by differentiating the thermal wind equation in the form (3.15) with respect to time t and using the azimuthal momentum equation and thermodynamic equation to eliminate the time derivatives. It is convenient to write the last two equations in the form

$$\frac{\partial v}{\partial t} + u(\zeta + f) + wS = \dot{V} \tag{3.47}$$

and

$$\frac{\partial \chi}{\partial t} + u\frac{\partial \chi}{\partial r} + w\frac{\partial \chi}{\partial z} = -\chi^2\dot{\theta} \tag{3.48}$$

where $\zeta = (1/r)(\partial(rv)/\partial r)$ is the relative vorticity and we have added a momentum source term $\dot{V}$ in the former equation for reasons that will emerge later. The time derivative of (3.10) is

$$g\frac{\partial}{\partial r}\frac{\partial \chi}{\partial t} + \frac{\partial}{\partial z}\left(C\frac{\partial \chi}{\partial t} + \chi\frac{\partial C}{\partial t}\right) = 0$$

and substitution of the time derivatives from (3.47) and (3.48) gives

$$g\frac{\partial}{\partial r}\left(u\frac{\partial \chi}{\partial r} + w\frac{\partial \chi}{\partial z} - Q\right) + \frac{\partial}{\partial z}\left[C\left(u\frac{\partial \chi}{\partial r} + w\frac{\partial \chi}{\partial z} - Q\right) + \chi\xi\left(u(\zeta + f) + wS - \dot{V}\right)\right] = 0$$

where $\chi = 1/\theta$ and $Q = -\chi^2\dot{\theta}$. Then

$$\frac{\partial}{\partial r}\left[g\frac{\partial \chi}{\partial z}w + g\frac{\partial \chi}{\partial r}u\right] +$$

$$\frac{\partial}{\partial z}\left[(\chi\xi(\zeta + f) + C\frac{\partial \chi}{\partial r})u + \frac{\partial}{\partial z}(\chi C)w\right] = g\frac{\partial Q}{\partial r} + \frac{\partial}{\partial z}(CQ) + \frac{\partial}{\partial z}(\chi\xi\dot{V})$$

or

$$\frac{\partial}{\partial r}\left[g\frac{\partial \chi}{\partial z}w - \frac{\partial}{\partial z}(\chi C)u\right] +$$

$$\frac{\partial}{\partial z}\left[(\chi\xi(\zeta + f) + C\frac{\partial \chi}{\partial r})u + \frac{\partial}{\partial z}(\chi C)w\right] = g\frac{\partial Q}{\partial r} + \frac{\partial}{\partial z}(CQ) + \frac{\partial}{\partial z}(\chi\xi\dot{V}) \tag{3.49}$$

using (3.15). Then substitution for u and w from Eqs. (3.46) into Eq. (3.49) gives

$$\frac{\partial}{\partial r}\left[g\frac{\partial \chi}{\partial z}\frac{1}{\rho r}\frac{\partial \psi}{\partial r} + \frac{\partial}{\partial z}(\chi C)\frac{1}{\rho r}\frac{\partial \psi}{\partial z}\right] -$$

$$\frac{\partial}{\partial z}\left[\left(\xi\chi(\zeta + f) + C\frac{\partial \chi}{\partial r}\right)\frac{1}{\rho r}\frac{\partial \psi}{\partial z} - \frac{\partial}{\partial z}(\chi C)\frac{1}{\rho r}\frac{\partial \psi}{\partial r}\right] = g\frac{\partial Q}{\partial r} + \frac{\partial}{\partial z}(CQ) + \frac{\partial}{\partial z}(\chi\xi\dot{V}) \tag{3.50}$$

This is called the *Sawyer-Eliassen equation* following the work of these two authors. The discriminant of the Sawyer-Eliassen equation is

$$D = -g\frac{\partial \chi}{\partial z}\left(\xi\chi(\zeta + f) + C\frac{\partial \chi}{\partial r}\right) - \left[\frac{\partial}{\partial z}(\chi C)\right]^2 \tag{3.51}$$

It can be shown that Eq. (3.50) is elliptic if $D > 0$.

The Sawyer-Eliassen equation contains three spatially-varying parameters characterizing:

- the *static stability*

$$N^2 = -g\frac{\partial ln\chi}{\partial z};$$

- the *inertial stability*

$$I^2 = \frac{1}{r^3}\frac{\partial M^2}{\partial r} = \xi(\zeta + f);$$

- the *baroclinicity*

$$B_1 = \frac{1}{r^3}\frac{\partial M^2}{\partial z} = \xi S.$$

It is instructive to examine the solutions of the Sawyer-Eliassen equation for point sources (i.e. azimuthal rings) of heat and azimuthal momentum that are shown in Fig. 3.10. The flow through the heat source follows a nearly vertical surface of constant absolute angular momentum, while that for a momentum source follows a nearly horizontal isentropic surface. For sources of heat and absolute angular momentum, the sense of the flow is upward and outward, respectively. For sinks the flow is reversed. The vortex axis lies to the left of the figure. In the warm-core system of panels (c) and (f), the warm anomaly that supports the slope of the constant absolute angular momentum and isentropic surfaces increases towards the upper left.

Figure 3.11 shows the secondary circulation induced by point sources of heat and absolute angular momentum in balanced, tropical-cyclone-like vortices in a partially bounded domain. These solutions can be obtained using the so-called method of images. Again the secondary circulation through a heat source is primarily vertical, and that through a momentum source is primarily horizontal. The streamlines form two counter-rotating cells of circulation (or gyres) that extend outside the source. There is a strong flow between these gyres and a weaker return flow on the outside. The flow emerges from the source, spreads outward through a large volume surrounding it, and converges back into it from below. Thus, compensating subsidence surrounds heat-induced updraughts and compensating inflow lies above and below momentum-induced outflow. The horizontal scale of the gyres is just the local Rossby length, so that the ratio of horizontal to vertical scale is N/I.

Radial gradients of absolute angular momentum of the primary circulation affect the radial scale of the dipoles just as the static stability affects their vertical scale. For a fixed static stability, the gyres tend to be elongated vertically when the inertial-stability parameter I^2 is large and elongated horizontally when I^2 is small. Vertical gradients of absolute angular momentum associated with the vertical shear of the primary circulation tilt the updraught through a heat source because the path of least resistance for the rising air lies along surfaces of constant absolute angular momentum. Likewise, horizontal temperature gradients associated with the vertical shear deflect the flow through momentum sources from the horizontal because the path of least resistance in this case lies along isentropic surfaces. Although the flow

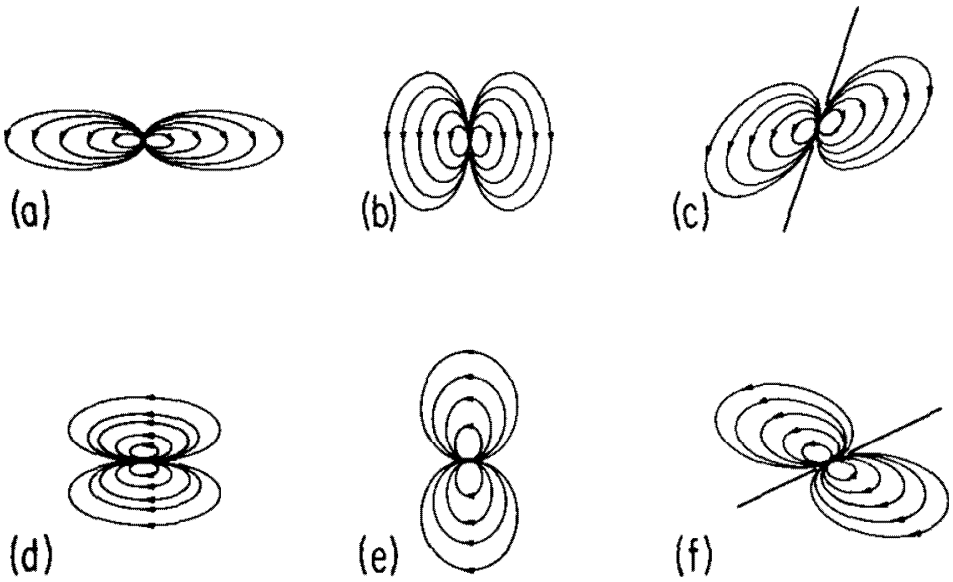

Figure 3.10: Streamfunction responses to point sources of: (a) Heat in a barotropic vortex with weak inertial stability, (b) heat in a barotropic vortex with strong inertial stability, (c) heat in a baroclinic vortex, (d) momentum in a barotropic vortex with weak inertial stability, (e) momentum in a barotropic vortex with strong inertial stability, and (f) momentum in a baroclinic vortex. (Based on Figs. 8, 9, 11, and 12 of (?).)

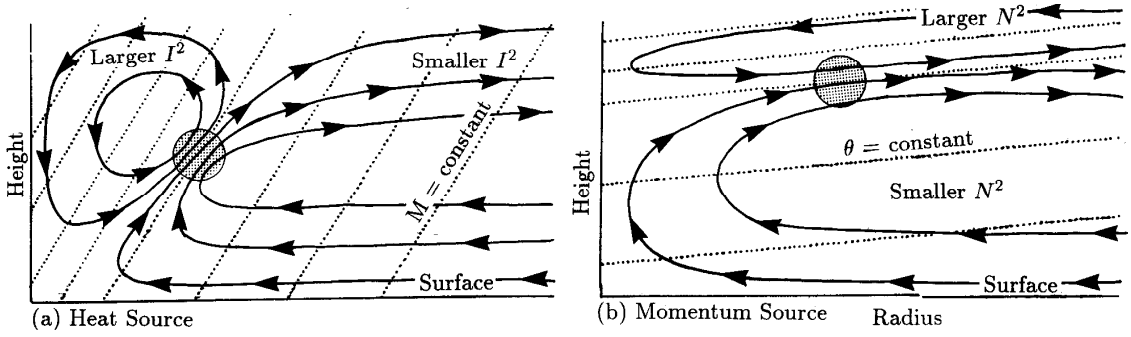

Figure 3.11: Secondary circulation induced in a balanced vortex by (a) a heat source and (b) a cyclonic momentum source showing the distortion induced by variation in inertial stability, I^2 and thermodynamic stability. N^2, and baroclinicity S^2. The strong motions through the source follow lines of constant angular momentum for a heat source and of constant potential temperature for a momentum source. From (?).

associated with a heat (momentum) source lies generally along the M-surface (θ-surface), it does have a small component across this surface. It is the advection by this component that causes evolution of the primary circulation. It can be shown that the swirling flow remains in approximate gradient-wind balance provided the time scale of the forcing is longer than the orbital period of the primary circulation about the vortex centre.

It turns out that the induced secondary circulation in balanced flows tend to cancel the direct effect of forcing. For example, the work done by expansion in the updraught induced by a heat source nearly balances the actual heating so that the increase in temperature is relatively small. Similarly, a momentum source produces outflow that advects compensating low values of absolute angular momentum from the central region of the vortex.

3.8 A balanced theory of vortex evolution

The establishment of the Sawyer-Eliassen equation is an important step in formulating a balanced theory for the evolution of an axisymmetric vortex. In such a theory we need prognostic equations for the evolution of the primary circulation, i.e. for the azimuthal wind and potential temperature. These are just the axisymmetric forms of Eqs. (3.2) and (3.5), i.e. Eqs. (3.47) and (3.48). Given expressions for $\dot{V}$ and $\dot{\theta}$ and initial conditions for v and θ, we can solve the Sawyer-Eliassen equation for the streamfunction of the secondary circulation, ψ, given suitable boundary conditions on this quantity. This streamfunction gives the secondary circulation that keeps v and θ in thermal-wind balance for short time interval, Δt. The corresponding radial and vertical wind components may be obtained from the expressions (3.46) and the density therein can be obtained, in principle, from (3.14).

3.8.1 The Sawyer-Eliassen equation and toroidal vorticity equation

The Sawyer-Eliassen equation is an approximate form of the local time derivative of equation for the toroidal vorticity $\eta = \partial u/\partial z - \partial w/\partial r$. Assuming the most general form of the continuity equation

$$\frac{\partial \rho}{\partial t} + \frac{1}{r}\frac{\partial}{\partial r}(r\rho u) + \frac{\partial}{\partial z}(\rho w) = 0$$

the toroidal vorticity equation may be written as

$$r\frac{D}{Dt}\left(\frac{\eta}{r\rho}\right) = \frac{1}{\rho}\frac{\partial C}{\partial z} + \frac{1}{\rho^2\chi}\left(\frac{\partial \chi}{\partial z}\frac{\partial p}{\partial r} - \frac{\partial \chi}{\partial r}\frac{\partial p}{\partial z}\right) \tag{3.52}$$

where $D/Dt \equiv \partial/\partial t + \mathbf{u}\cdot\nabla$ and $\eta/(r\rho)$ is a 'potential toroidal vorticity', where the analogous 'depth' is 'r', the radius of a toroidal vortex ring (see appendix). If

thermal wind balance exists, the right-hand-side of (3.57) may be written as

$$\frac{1}{\rho\chi}\left(g\frac{\partial\chi}{\partial r}+\frac{\partial}{\partial z}(C\chi)\right).$$

Then the time derivative of (6.41) is

$$\frac{\partial}{\partial t}\left[r\frac{D}{Dt}\left(\frac{\eta}{r\rho}\right)\right]=\frac{\partial}{\partial t}\left[\frac{1}{\rho\chi}\left(g\frac{\partial\chi}{\partial r}+\frac{\partial}{\partial z}(C\chi)\right)\right] \tag{3.53}$$

The right-hand-side of (3.53) gives the Sawyer-Eliassen equation when the thermal wind equation (3.10) is satisfied for all time. Then consistency requires that the left-hand-side is identically zero.

Exercise 3.10 Show now that the quantity D in Eq. (3.51) is proportional to the Ertel potential vorticity defined by Eq. (3.51). Hint: show first that for a symmetric vortex with tangential wind speed distribution $v(r,z)$, $\omega+\mathbf{f}=-(\partial v/\partial z)\hat{\mathbf{r}}+(\zeta+f)\hat{\mathbf{z}}$ and $\nabla\theta=-(1/\chi^2)\nabla\chi=-(1/\chi^2)[(\partial\chi/\partial r)\hat{\mathbf{r}}+(\partial\chi/\partial z)\hat{\mathbf{z}}]$ so that

$$P=\frac{1}{\rho\chi^2}\left[\frac{\partial v}{\partial z}\frac{\partial\chi}{\partial r}-(\zeta+f)\frac{\partial\chi}{\partial z}\right]$$

Exercise 3.11 Show that the forcing term for ψ can be expressed in terms of generalized buoyancy. Hint: show first that the forcing term in Eq. (3.51)can be written:

$$F=-g\frac{\partial}{\partial r}\left(\frac{1}{\theta^2}\frac{d\theta}{dt}\right)-\frac{\partial}{\partial z}\left(C\frac{1}{\theta^2}\frac{d\theta}{dt}\right)$$

and deduce that that

$$F\approx\frac{1}{\Theta}\hat{\theta}.\nabla\wedge\frac{d\mathbf{b_e}}{dt}. \tag{3.54}$$

Exercise 3.12 Starting from the Boussinesq system of equations, show that the Sawyer-Eliassen equation takes the form

$$\frac{\partial}{\partial r}\left[\left(N^2+\frac{\partial b}{\partial z}\right)\frac{1}{r}\frac{\partial\psi}{\partial r}-\frac{S\xi}{r}\frac{\partial\psi}{\partial z}\right]+\frac{\partial}{\partial r}\left[\frac{I^2}{r}\frac{\partial\psi}{\partial z}-\frac{S\xi}{r}\frac{\partial\psi}{\partial r}\right]=-\frac{\partial\dot{B}}{\partial r}-\frac{\partial}{\partial z}(\xi\dot{V}), \tag{3.55}$$

where $dotB$ is the source of buoyancy in the Boussinesq form of the thermodynamic equation and I^2 is defined in Eq. (3.33) (see also Ex. 3.5).

3.8.2 Buoyancy relative to a balanced vortex

Tropical cyclones are rapidly-rotating warm-cored vortices and the warm core is therefore positively buoyant relative to the environment. However, we have seen that

on the cyclone scale, hydrostatic and gradient-wind balance exist to a good approximation and the radial density (or buoyancy) gradient is related by the thermal-wind equation to the decay in the mean tangential circulation and density with height. Clearly much of the radial gradient of buoyancy force cannot be thought of as being "available" for "driving" a secondary (or toroidal) circulation of the vortex that is necessary for vortex amplification. Nevertheless, hydrostatic balance may be a poor approximation in individual convective clouds and a pertinent question is whether these clouds have significant local (unbalanced) buoyancy, which in turn might play an important role in the dynamics of storm intensification. To address this question it is necessary to define the perturbation pressure and perturbation density relative to some vortex-scale pressure and density distributions. The simplest case is when the primary vortex is approximately steady and axisymmetric. Then we may take reference distributions $p_{ref}(r,z)$ and $\rho_{ref}(r,z)$, respectively, that are in thermal wind balance with the tangential flow field $v(r,z)$. We saw how to do this in section 3.2 using the method of characteristics. We may use $\rho_{ref}(r,z)$ and $p_{ref}(r,z)$ as alternative reference quantities to define the buoyancy force in Eq. (1.27) without affecting the derivation of this equation. We denote the generalized buoyancy force so calculated by $\mathbf{b_B}$. It follows that $\mathbf{b_B} \equiv \mathbf{0}$ in the axisymmetric balanced state, whereas, if the reference pressure and density at $r = R$ are used, $\mathbf{b}$ equals some nonzero function $\mathbf{b_0}(r,z)$. Clearly, the partition of force between perturbation pressure gradient and buoyancy will be different for the reference state characterized by $\rho_0(r,z)$ and $p_0(r,z)$ and interpretations of the dynamics will be different also, albeit equivalent to those using the more conventional reference quantities that depend on height only.

In the more general case, when the vortex structure has marked asymmetries and/or is evolving in time, it is necessary to allow for the azimuthal and/or time variations of the reference state.

3.8.3 Buoyancy in axisymmetric balanced vortices

Axisymmetric balanced models of tropical cyclone intensification appear to capture many important observed features of tropical cyclone behaviour. However, in an axisymmetric model that assumes exact thermal wind balance, $\mathbf{b_B}(r,z,t) \equiv \mathbf{0}$ and the corresponding $\partial p'/\partial z \equiv 0$, even though there may be heat sources or sinks present that generate buoyancy $\mathbf{b}$. It is clear from the foregoing discussion that any diabatic heating or cooling in such models is incorporated directly into the balanced state, changing $\mathbf{b}(r,z,t)$, while $\mathbf{b_B}(r,z,t)$ remains identically zero by definition. Obviously, nonzero values of $\mathbf{b_B}$ relate to *unbalanced motions* provided that the appropriate reference state as defined above has been selected for the definition of buoyancy at any given time. It may be helpful to think of $\mathbf{b}$ as characterizing the *system buoyancy* and $\mathbf{b_B}$ as characterizing the *local buoyancy*.

3.9 Origins of buoyancy in tropical cyclones

Tropical cyclones intensify when, as a direct or indirect result of latent heat release, the buoyancy b in the core increases. To a first approximation, the direct effect of latent heat release in saturated ascending air, such as in the eyewall clouds, or in the cores of individual convective clouds, is to maintain the air close to the moist adiabat from which the updraught originates. The indirect effect of latent heat release is to produce subsidence (or at least reduce the rate-of-ascent) in clear-air regions adjacent to (i.e. within a local Rossby length of) deep convection. There is observational evidence and evidence from model studies that, again to a first approximation, the clear air properties are adjusted towards the same saturation moist adiabat as in the neighbouring convective cores, albeit in this case to one calculated reversibly. In either case, the thermal structure of the troposphere in a mature tropical cyclone, and thereby the radial distribution of buoyancy, would be determined largely by the radial distribution of moist entropy at the top of the subcloud layer, at least in regions of ascent. This view relates essentially to the generation of system buoyancy.

Need to move references here to further reading:

The extent to which local (unbalanced) buoyancy is produced will depend amongst other things on the rate at which the buoyancy is generated and the scale on which it is generated. For example, the simulations by (**?**) indicate that much of the eyewall updraft mass flux occurs within small-scale updrafts that are locally buoyant relative to the broad-scale thermal field of the vortex. A recent examination of the high resolution cloud resolving numerical simulation of the formation of Hurricane Diana (1984) has shown how buoyant cores growing in the rotation-rich environment of an incipient storm produce intense cyclonic vorticity anomalies in the lower troposphere by vortex-tube stretching (**?**). These intense vorticity anomalies subsequently merge and axisymmetrize to intensify the balanced circulation of the incipient mesoscale vortex (**?**); (**?**); (**?**). In this case, subsidence warming is not the primary means for generating the cyclone's warm core. Rather, the warm core temperature that materializes within the developing mesoscale vortex results from the tendency of the high vorticity cores of the buoyant plumes to 'trap' the heat releases by the condensation process, as one might anticipate from local Rossby adjustment considerations (Schubert *et al.* 1980, Sec. 9) and quasi-balanced dynamics within enhanced vortical regions (**?**), Montgomery *et al.* 2003.

3.10 Appendix to Chapter 1

3.10.1 The toroidal vorticity equation

The λ-component of vorticity, or toroidal vorticity is

$$\eta = \frac{\partial u}{\partial z} - \frac{\partial w}{\partial r} \tag{3.56}$$

The equation for η is derived as follows. Consider

$$\frac{\partial \eta}{\partial t} = \frac{\partial}{\partial t}\left(\frac{\partial u}{\partial z} - \frac{\partial w}{\partial r}\right) = \frac{\partial}{\partial z}\left(\frac{\partial u}{\partial t}\right) - \frac{\partial}{\partial r}\left(\frac{\partial w}{\partial t}\right)$$

This expression may be written

$$\frac{\partial \eta}{\partial t} = \frac{\partial}{\partial z}\left(-\mathbf{u}\cdot\nabla u + C - \frac{1}{\rho}\frac{\partial p}{\partial r} + F_u\right) - \frac{\partial}{\partial r}\left(-\mathbf{u}\cdot\nabla w - \frac{1}{\rho}\frac{\partial p}{\partial z} + F_w\right),$$

where, for completeness frictional stresses F_u, F_w, are included in the momentum equations. This equation reduces to

$$\frac{\partial \eta}{\partial t} = \frac{\partial C}{\partial z} + \frac{\partial}{\partial r}\left(\frac{1}{\rho}\right)\frac{\partial p}{\partial z} - \frac{\partial}{\partial z}\left(\frac{1}{\rho}\right)\frac{\partial p}{\partial r} + \frac{\partial}{\partial r}\left(\mathbf{u}\cdot\nabla w\right) - \frac{\partial}{\partial z}\left(\mathbf{u}\cdot\nabla u\right) + \frac{\partial F_u}{\partial z} - \frac{\partial F_w}{\partial r},$$

or

$$\frac{\partial \eta}{\partial t} + \mathbf{u}\cdot\nabla\eta = \frac{\partial C}{\partial z} + \frac{1}{\rho^2}\left(\frac{\partial \rho}{\partial z}\frac{\partial p}{\partial r} - \frac{\partial \rho}{\partial r}\frac{\partial p}{\partial z}\right) + \frac{\partial \mathbf{u}}{\partial r}\cdot\nabla w - \frac{\partial \mathbf{u}}{\partial z}\cdot\nabla u + \frac{\partial F_u}{\partial z} - \frac{\partial F_w}{\partial r}.$$

Now

$$\ln\theta = \kappa\ln p^* - (1-\kappa)\ln p - \ln\rho = -\ln\chi$$

so that

$$(1-\kappa)\frac{dp}{p} + \frac{d\rho}{\rho} = \frac{d\chi}{\chi}$$

Then

$$\frac{1}{\rho^2}\left(\frac{\partial \rho}{\partial z}\frac{\partial p}{\partial r} - \frac{\partial \rho}{\partial r}\frac{\partial p}{\partial z}\right) = \frac{1}{\rho\chi}\left(\frac{\partial \chi}{\partial z}\frac{\partial p}{\partial r} - \frac{\partial \chi}{\partial r}\frac{\partial p}{\partial z}\right)$$

Again

$$\frac{\partial \mathbf{u}}{\partial x}\cdot\nabla w - \frac{\partial \mathbf{u}}{\partial z}\cdot\nabla u = \left(\frac{\partial u}{\partial r} + \frac{\partial w}{\partial z}\right)\left(\frac{\partial w}{\partial r} - \frac{\partial u}{\partial z}\right),$$

but the continuity equation now gives

$$\frac{\partial u}{\partial r} + \frac{\partial w}{\partial z} = -\frac{u}{r} - \frac{1}{\rho}\left(\frac{\partial \rho}{\partial t} + u\frac{\partial \rho}{\partial r} + w\frac{\partial \rho}{\partial z}\right) = -\frac{u}{r} + \rho\frac{D}{Dt}\left(\frac{1}{\rho}\right),$$

where $D/Dt \equiv \partial/\partial t + \mathbf{u}\cdot\nabla$. Thus the toroidal vorticity equation is

$$\frac{\partial \eta}{\partial t} + \mathbf{u}\cdot\nabla\eta = \frac{\partial C}{\partial z} + \frac{1}{\rho\chi}\left(\frac{\partial \chi}{\partial z}\frac{\partial p}{\partial r} - \frac{\partial \chi}{\partial r}\frac{\partial p}{\partial z}\right) + \left[\frac{u}{r} + \rho\frac{D}{Dt}\left(\frac{1}{\rho}\right)\right]\eta + \frac{\partial F_u}{\partial z} - \frac{\partial F_w}{\partial r},$$

or

$$r\frac{D}{Dt}\left(\frac{\eta}{r\rho}\right) = \frac{1}{\rho}\frac{\partial C}{\partial z} + \frac{1}{\rho^2\chi}\left(\frac{\partial \chi}{\partial z}\frac{\partial p}{\partial r} - \frac{\partial \chi}{\partial r}\frac{\partial p}{\partial z}\right) + \frac{1}{\rho}\left(\frac{\partial F_u}{\partial z} - \frac{\partial F_w}{\partial r}\right), \tag{3.57}$$

3.11 Further reading for Chapter 1

(?) and (?)
(?)
(?); Xu and Emanuel (1989)
(?)
(?)

Chapter 4

Vortex Intensification

To understand spin-up of a tropical cyclone it is instructive to consider first the spin-down problem, which requires a consideration of frictional effects. We examine first the essential dynamics of the problem and proceed then to a scale analysis of the equations with the friction terms included.

4.1 Spin-down of a rotating vortex

The classic vortex spin down problem considers the evolution of an axisymmetric vortex above a rigid boundary normal to the axis of rotation. We will show that the spin down is intimately connected to the Coriolis torques associated with the secondary circulation induced by friction. The direct effect of the frictional diffusion of momentum to the surface is of secondary importance in the parameter regimes relevant to tropical cyclones.

In a shallow layer of air near the surface, typically 500 - 1000 m deep, frictional stresses reduce the tangential wind speed and thereby the centrifugal and Coriolis forces, while it can be shown that the force associated with the radial increase of pressure remains largely unchanged. We call this layer the friction layer. The result of the force imbalance is a net inward force that drives air parcels inwards in this layer. One can demonstrate this effect by placing tea leaves in a beaker of water and vigorously stirring the water to set it in rotation. After a short time the tea leaves congregate near the bottom of the beaker near the axis as shown in Fig. 4.1: they are swept there by the inflow in the friction layer. Slowly the rotation in the beaker declines because the inflow towards the rotation axis in the friction layer is accompanied by radially-outward motion above this layer. The depth of the friction layer depends on the viscosity of the water and the rotation rate and is typically only on the order of a millimetre or two in this experiment. Because the water is rotating about the vertical axis, it possess angular momentum about this axis. Here angular momentum is defined as the product of the tangential flow speed and the radius. As water particles move outwards above the friction layer, they conserve their angular momentum and as they move to larger radii, they spin more slowly.

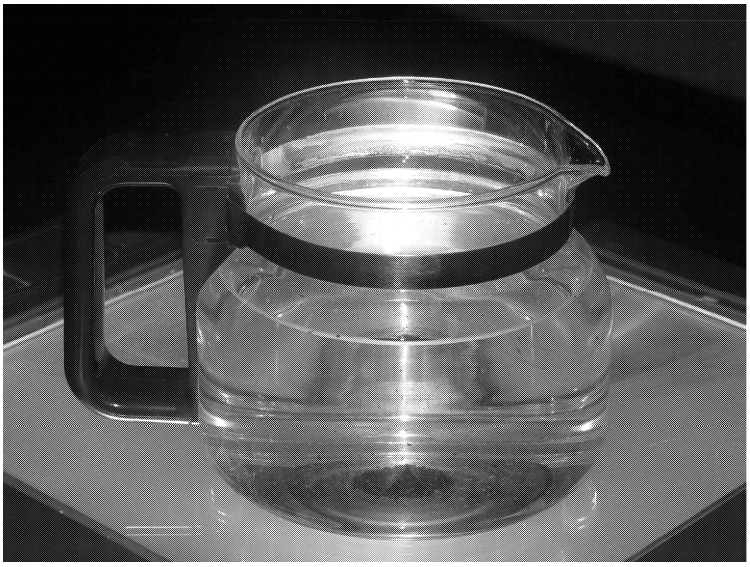

Figure 4.1: The beaker experiment showing the effects of frictionally-induced inflow near the bottom after the water has been stirred to produce rotation. This inflow carries tea leaves to form a neat pile near the axis of rotation.

The same process would lead to the decay of a hurricane if the frictionally-induced outflow were to occur just above the friction layer, as in the beaker experiment. What then prevents the hurricane from spinning down, or, for that matter, what enables it to spin up in the first place? Clearly, if it is to intensify, there must be a mechanism capable of drawing air inwards above the friction layer, and of course, this air must be rotating about the vertical axis and possess angular momentum so that as it converges towards the axis it spins faster. The only conceivable mechanism for producing inflow above the friction layer is the upward "buoyancy force" in the clouds, the origins of which we examine below.

4.2 Scale analysis of the equations with friction

We repeat now the scale analysis of the dynamical equations (3.1) - (3.3) with the friction terms $K(\nabla^2 u, \nabla^2 v, \nabla^2 w)$ added to the right-hand-sides. We have assumed a particularly simple form for friction with K an eddy diffusivity, assumed to be constant. We assume that the air is *homogeneous* and that the motion is axisymmetric and define velocity scales (U, V, W), length scales (R, Z), and an advective time scale $T = U/R$ as before. Now we assume that p is perturbation pressure and take Δp to be a scale for changes in this quantity. The continuity equation, (3.4), yields the same relation between $W/Z \sim U/R$ as before. Then the terms in Eqs. (3.1) to (3.3) have nondimensional scales as shown in Table 4.1.

As in section 3.5 we divide terms in line (2a) by V^2/R to obtain those in line (2b) and divide terms in line (3a) by UV/R to obtain those in line (3b). The

terms in line (4a) are divided by g to obtain those in line (4b). The terms in lines (b) are then nondimensional. We define a *Reynolds number*, $R_e = VZ/K$, which is a nondimensional parameter that characterizes the importance of the inertial to frictional terms, and an *aspect ratio* $A = Z/R$, that measures the ratio of the boundary-layer depth to the radial scale.

u-momentum

$$\frac{\partial u}{\partial t} \quad +u\frac{\partial u}{\partial r} \quad +w\frac{\partial u}{\partial z} \quad -\frac{v^2}{r} \quad -fv \quad = \quad -\frac{1}{\rho}\frac{\partial p}{\partial r} \quad +K\nabla_h^2 u \quad +K\frac{\partial^2 u}{\partial z^2} \qquad (4.1)$$

$$\frac{U}{T} \quad \frac{U^2}{R} \quad W\frac{U}{Z} \quad \frac{V^2}{R} \quad fV \quad \frac{\Delta p}{\rho R} \quad K\frac{U}{R^2} \quad K\frac{U}{Z^2} \qquad (1a)$$

$$S^2 \quad S^2 \quad S^2 \quad 1 \quad \frac{1}{Ro} \quad \frac{\Delta p}{\rho V^2} \quad SA^2R_e^{-1} \quad SR_e^{-1} \qquad (1b)$$

v-momentum

$$\frac{\partial v}{\partial t} \quad +u\frac{\partial v}{\partial r} \quad +w\frac{\partial v}{\partial z} \quad +\frac{uv}{r} \quad +fu \quad = \quad +K\nabla_h^2 v \quad +K\frac{\partial^2 v}{\partial z^2} \qquad (4.2)$$

$$\frac{V}{T} \quad U\frac{V}{R} \quad W\frac{V}{Z} \quad U\frac{V}{R} \quad fU \quad K\frac{V}{R^2} \quad K\frac{V}{Z^2} \qquad (2a)$$

$$S \quad S \quad S \quad S \quad \frac{S}{Ro} \quad A^2R_e^{-1} \quad R_e^{-1} \qquad (2b)$$

w-momentum

$$\frac{\partial w}{\partial t} \quad +u\frac{\partial w}{\partial r} \quad +w\frac{\partial w}{\partial z} \quad = \quad -\frac{1}{\rho}\frac{\partial p}{\partial z} \quad +K\nabla_h^2 w \quad +K\frac{\partial^2 w}{\partial z^2} \qquad (4.3)$$

$$\frac{W}{T} \quad \frac{UW}{R} \quad \frac{WW}{Z} \quad \frac{\Delta p}{\rho Z} \quad K\frac{W}{R^2} \quad K\frac{W}{Z^2} \qquad (3a)$$

$$S^2A^2 \quad S^2A^2 \quad S^2A^2 \quad \frac{\Delta p}{\rho V^2} \quad SA^3R_e^{-1} \quad SAR_e^{-1} \qquad (3b)$$

Table 4.1: Scaling of the terms in Eqs. (3.1) to (3.3) with frictional terms added. Here $\nabla_h^2 = (\partial/\partial r)(r\partial/\partial r)$.

Typically, the boundary layer is thin, not more than 500 m to 1 km in depth and the aspect ratio is small compared with unity. Moreover, typical values of K are on the order of 10 m s^{-2}. Therefore taking $V = 50$ m s^{-1}, $R = 50$ km, and $Z = 500$ m,

$R_e = 2.5 \times 10^3$ and $A = 10^{-2}$. It follows from line (3b) in Table 4.1 that $\Delta p/(\rho V^2) \approx \max(S^2A^2, SAR_e^{-1}) = 4 \times 10^{-4}$, assuming that $S \approx 1$ in the boundary layer. Thus the vertical variation of p across the boundary layer is only a tiny fraction of the radial variation of p above the boundary layer. In other words, to a close approximation, the radial pressure gradient within the boundary layer is the same as that above the boundary layer.

From lines (1a) and (2a) in Table 4.1, we see that a vertical scale Z which makes friction important compared with the other large terms is $(K/f)^{\frac{1}{2}}$ if $Ro << 1$ and $(K/(V/R))^{\frac{1}{2}}$ if $Ro \approx 1$ or larger. The former result gives us the appropriate scaling for the Ekman layer.

4.3 The Ekman boundary layer

The scale analysis of the u- and v-momentum equations in Table 4.1 show that for small Rossby numbers ($Ro << 1$), there is an approximate balance between the net Coriolis force and the diffusion of momentum, expressed by the equations:

$$f(v_g - v) = K\frac{\partial^2 u}{\partial z^2} \tag{4.1}$$

and

$$fu = K\frac{\partial^2 v}{\partial z^2}, \tag{4.2}$$

where we have used the fact deduced from the scale analysis of the w-momentum equation that the horizontal pressure gradient in the boundary layer is essentially the same as that above it. Thus we have replaced the radial pressure gradient in Eq. (4.1) by the geostrophic wind, v_g, above the boundary layer. We assume also that the radial flow above the boundary layer is zero.

Equations (4.1) and (4.2) are linear in u and v and may be readily solved by setting $V = v + iu$, where $i = \sqrt{(-1)}$. Then they reduce to the single differential equation

$$K\frac{d^2V}{dz^2} - ifV = -ifV_g, \tag{4.3}$$

where $V_g = v_g$. This equation has the particular integral $V = V_g$ and there are two complementary functions proportional to $\exp(\pm(1-i)z/\delta)$, where $\delta = \sqrt{2K/f}$. Since we require a solution that remains bounded as $z \to \infty$ we reject the solution with a positive exponent so that the solution has the form

$$V = V_g[1 - A\exp(-(1-i)z/\delta),] \tag{4.4}$$

where A is a complex constant determined by a suitable boundary condition at $z = 0$. For a laminar viscous flow, the flow at $z = 0$ is zero giving $A = 1$. This is the classical Ekman solution. The profiles of u and v are shown in Fig. 4.2a and the hodograph thereof is the Ekman spiral shown in Fig. 4.2b. Two interesting features of the

solution are the fact that the boundary-layer thickness, measured by δ is a constant and there are regions in the boundary layer where the flow is supergeostrophic, i.e. $v > V_g$. These are unusual features of boundary layers which are typically regions where the flow is retarded and which grow in thickness downstream as more and more fluid is retarded. In the Ekman layer, the fluid that is retarded in the downstream direction, but is re-energized in the cross-stream direction by the net pressure gradient force in that direction. The latter occurs because friction reduces the Coriolis force in the boundary layer whereas the radial pressure gradient remains effectively unchanged. The height range where the flow is supergeostrophic is one in which the net radial flow is outwards. The fact that the radial flow is inwards over this range is a result of the upward diffusion of u-momentum, which is largest at low levels.

The existence of a region of supergeostrophic winds may be made plausible by considering the spin-down problem in which there is initially a uniform geostrophic flow, V_g, at large radius. If the frictional stress is switched on at the surface at time zero, the tangential flow will be reduced near the surface leading to a net pressure gradient in the radial direction. This will drive a radial flow that is largest near the surface where the net pressure gradient is largest. The Coriolis force acting on the radial flow will tend to accelerate the tangential flow as part of an inertial oscillation. Whether or not the tangential flow becomes supergeostrophic after some time will depend subtly on the vertical diffusion of momentum in the radial and tangential directions, but the Ekman solution indicates that it does.

The classical Ekman solution with a no-slip boundary condition at the surface is a poor approximation in the atmospheric boundary layer. A better one is to prescribe the surface stress, τ_0, as a function of the near-surface wind speed, normally taken to be the wind speed at a height of 10 m, and a drag coefficient, C_D. The condition takes the form

$$\frac{\tau_0}{\rho} = K\frac{\partial V}{\partial z} = C_D\,|V|\,V \tag{4.5}$$

and we shall apply it at $z = 0$ instead of 10 m. Substituting (4.4) into (4.10) and tidying up the equation gives

$$(1-i)A = \nu|1-A|(1-A) \tag{4.6}$$

where $\nu = C_D Re$ and $Re = V_g\delta/K$ is a Reynolds' number to the boundary layer. Setting $1 - A = Be^{i\beta}$ gives after a little algebra an equation for B and an expression for β in terms of B (see Exercise 4.1). The equation for B may be solved using a Newton-Rapheson algorithm. Profiles of $u(z)$ and $v(z)$ obtained for values $V_g = 10$ m s^{-1}, $f = 10^{-4}$ s^{-1}, $K = 10$ m^2 s^{-2} and $C_D = 0.002$ are shown in Fig. 4.2a also and the corresponding hodograph is shown in Fig. 4.2b. For these values, the boundary layer depth scale, $\delta = 450$ m and the surface values of v and u are about $0.7V_g$ and $0.2V_g$, respectively.

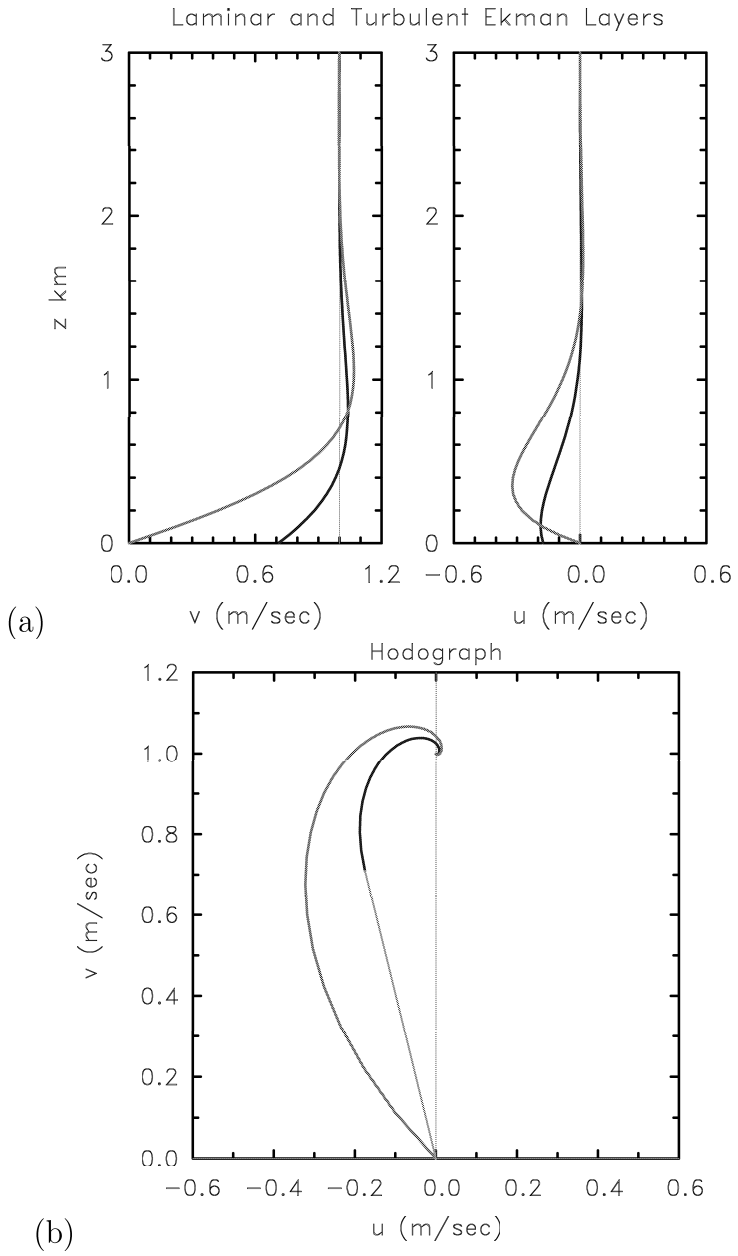

Figure 4.2: (a) Vertical profiles of tangential and radial wind components for the Ekman layer (red curves) and the modified Ekman layer based on a surface drag formulation (blue curves). (b)Hodograph of the two solutions showing the spiral of the wind vector.

4.4 The modified Ekman layer

From the scale analysis in Table 4.1, the full $u-$ and $v-$momentum equations in the boundary layer are:

$$\frac{\partial u}{\partial t} + u\frac{\partial u}{\partial r} + w\frac{\partial u}{\partial z} + \frac{V^2 - v^2}{r} + f(V - v) = K\frac{\partial^2 u}{\partial z^2}, \tag{4.7}$$

$$\frac{\partial v}{\partial t} + u\frac{\partial v}{\partial r} + w\frac{\partial v}{\partial z} + \frac{uv}{r} + fu = K\frac{\partial^2 v}{\partial z^2}, \tag{4.8}$$

where $V(r)$ is the gradient wind speed above the boundary layer. With the substitution $v = V(r) + v'$, these equations become:

$$\frac{\partial u}{\partial t} + u\frac{\partial u}{\partial r} + w\frac{\partial u}{\partial z} - \frac{v'^2}{r} - \left(\frac{2V}{r} + f\right)v' = K\frac{\partial^2 u}{\partial z^2} \tag{4.9}$$

$$\frac{\partial v'}{\partial t} + u\frac{\partial v'}{\partial r} + w\frac{\partial v'}{\partial z} + \frac{uv'}{r} + \left(\frac{dV}{dr} + \frac{V}{r} + f\right)u = K\frac{\partial^2 v'}{\partial z^2} \tag{4.10}$$

We carry out now a scaling of the terms in these equations as shown in Table 4.2. Let U, V^* and V' be scales for u, V and v', respectively. Examination of the u- and v-profiles for the case with a surface drag coefficient in Fig. 4.2 suggests that $U \approx V' \approx 0.2V^* - 0.3V^*$. Accordingly we assume that $U = V'$ and define $S^* = U/V^*$, which may be as large as 0.3.

With the background gradient wind balance removed, there is less of a scale separation between the various terms in the boundary-layer equations. If $\zeta*$ is regarded as small compared with unity, we could linearize Eqs. (4.9) and (4.9) to obtain

$$-\left(\frac{2V}{r} + f\right)v' = K\frac{\partial^2 u}{\partial z^2}, \tag{4.11}$$

$$\left(\frac{dV}{dr} + \frac{V}{r}\right)u = K\frac{\partial^2 v'}{\partial z^2}. \tag{4.12}$$

It is interesting to examine this approximation even though the neglect of terms of magnitude 0.2-0.3 compared with unity is unlikely to be very accurate. For one thing the equations (4.11) and (4.12) are relatively easy to solve and thy are a generalization of the Ekman layer theory derived in the previous subsection. The difference in the coefficients of v' and u on the left-hand-side of the equations precludes the method used for the Ekman equations 4.1 and 4.2. Now we differentiate one of the equations twice with respect to z and use the remaining equation to eliminate either u or v'. Then each of these quantities satisfies the equation

$$\frac{\partial^4 x}{\partial z^4} + \frac{I^2 x}{K^2} = 0 \tag{4.13}$$

The solutions have the form $x = ae^{\alpha z}$ where $\alpha^4 = (I^2/K^2)e^{i\pi + 2n\pi i}$, $(n = 0,\ 1,\ 2,\ 3)$, and a is a constant. Thus the four roots are $\alpha = \pm(1 \pm i)/\delta$, where $\delta = (2K/I)^{1/2}$ is

u-momentum

$$\frac{\partial u}{\partial t} \quad +u\frac{\partial u}{\partial r} \quad +w\frac{\partial u}{\partial z} \quad -\frac{v'^2}{r} \qquad -\left(\frac{2V}{r}+f\right)v' \quad = \quad +K\frac{\partial^2 u}{\partial z^2} \qquad (4.9)$$

$$\frac{U}{T} \quad \frac{U^2}{R} \quad W\frac{U}{Z} \quad \frac{V'^2}{R} \qquad \frac{2V^*V'}{R} \quad fV' \qquad K\frac{U}{Z^2} \qquad (1a)$$

$$S^* \quad S^* \quad S^* \quad S^* \qquad 2 \quad \frac{1}{Ro} \qquad R_e^{-1}\frac{R}{Z} \qquad (1b)$$

v-momentum

$$\frac{\partial v'}{\partial t} \quad +u\frac{\partial v'}{\partial r} \quad +w\frac{\partial v'}{\partial z} \quad +\frac{uv'}{r} \quad +\left(\frac{\partial V}{\partial r}+\frac{V}{r}+f\right)u \quad = \quad +K\frac{\partial^2 v'}{\partial z^2} \qquad (4.10)$$

$$\frac{V'}{T} \quad U\frac{V'}{R} \quad W\frac{V'}{Z} \quad \frac{UV'}{R} \qquad \frac{VU}{R} \quad \frac{VU}{R} \quad fU \qquad K\frac{V'}{Z^2} \qquad (2a)$$

$$S^* \quad S^* \quad S^* \quad S^* \qquad 1 \quad 1 \quad \frac{1}{Ro} \qquad R_e^{-1}\frac{R}{Z} \qquad (2b)$$

Table 4.2: Scaling of the terms in Eqs. (4.9) to (4.10). Here $S^* = U/V^* = V'/V^*$, $Ro = V^*/(fR)$ and $Re = VZ/K$.

the boundary-layer scale thickness. The solutions for v' and u which decay as $z \to \infty$ can be written succinctly in matrix form

$$\begin{pmatrix} v' \\ u \end{pmatrix} = Ve^{-z/\delta} \begin{pmatrix} a_1 & a_2 \\ b_1 & b_2 \end{pmatrix} \begin{pmatrix} \cos^{z/\delta} \\ \sin^{z/\delta} \end{pmatrix} \qquad (4.14)$$

where a_1, a_2, b_1, b_2 are constants. Two relations between these constants may be determined by applying the boundary condition (4.5), remembering that this applies to the total surface wind field $(V+v', u)$. Two further relationships may be obtained by substituting for v' and u in Eq. (4.12). The details form the basis of Exercise (4.2). Given a radial profile of $V(r)$ such as that shown in Fig. 4.3, it is possible to calculate the full boundary-layer solution $(u(r,z), v(r,z), w(r,z))$ on the basis of Eq. (4.14). The vertical velocity, $w(r,z)$ is obtained by integrating the continuity equation (see Exercise 4.3).

Figure 4.4 shows the isotachs of u and v and the vertical velocity at the top of the boundary layer for the tangential wind profile shown in Fig. 4.3. It shows also the radial variation of the boundary layer depth scale, δ. Note that δ decreases markedly with decreasing radius, while the inflow increases. The maximum inflow occurs in this case at a radius of 90 km, 50 km outside the radius of maximum wind speed

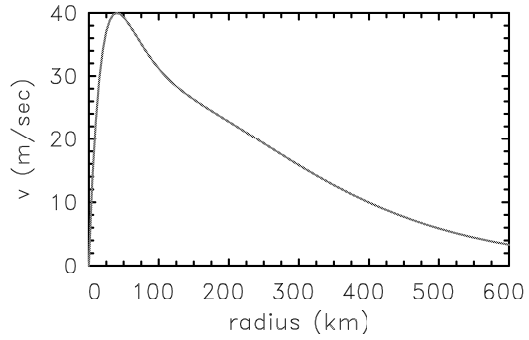

Figure 4.3: Tangential wind profile as a function of radius used in the calculations for Fig. 4.4.

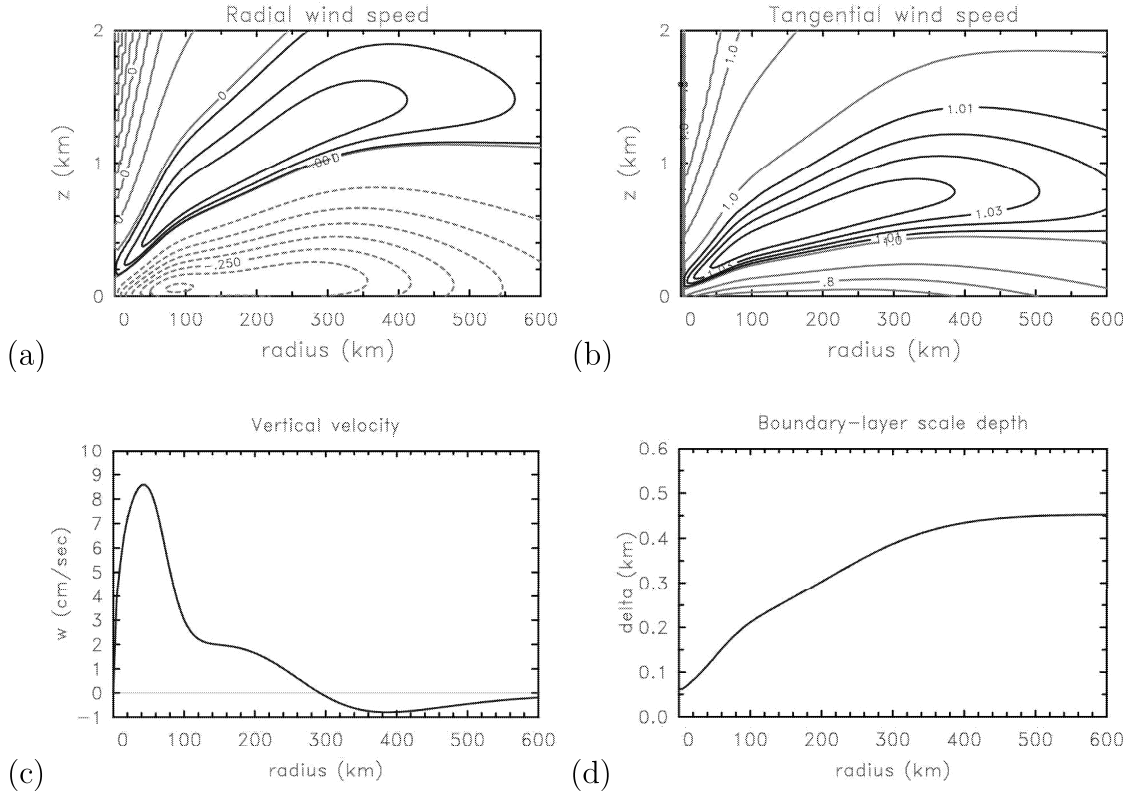

Figure 4.4: Isotachs of (a) radial wind, and (b) tangential wind in the $r - z$ plane obtained by solving Eqs. (4.11) and (4.12) with the tangential wind profile shown in Fig. 4.4. (c) Vertical velocity at the top of the boundary layer, and (d) radial variation of boundary-layer scale depth, $\delta(r)$.

above the boundary layer, r_m. In contrast, the maximum vertical velocity at "large heights" peaks just outside r_m. There is a region of weak outflow above the inflow layer coinciding roughly with the region where tangential flow becomes subgradient.